I. AN ATTEMPT TO PRODUCE BOTH THICK AND THINNED FLOWING SUPERFLUID FILMS

II. A STUDY OF THE FEASIBILITY OF VERIFYING LIFSHITZ'S THEORY OF VAN DER WAALS FORCE FOR A METALLIC SURFACE

III. THE ELECTROHYDRODYNAMIC INSTABILITY OF THE SUPER-THICK HELIUM FILM

Thesis by
Daniel S. W. Kwoh

In Partial Fulfillment of the Requirements
for the degree of
Doctor of Philosophy

California Institute of Technology
Pasadena, California
1979

(Submitted May 7, 1979)

To Cassandra and my parents

ACKNOWLEDGEMENTS

This work would have been impossible if it were not for the assistance extended to me by many different sources. In particular, my gratitude goes to

Professor David Goodstein, my supervisor, whose infinite patience and encouragement have been most supportive even when the experiment is not going so well, and whose deep insights have taught me how to think as a scientist,

Dr. Peter Mason of the Low Temperature Physics Group of the Jet Propulsion Laboratory, who has graciously allowed me to monopolize their He^3 refrigerator for so many years and who has responded to my many whims and wishes for equipment and technical assistance always with expedition,

Dr. Milton Cole, who suggested the idea of virtually raising the bath level by a dc bias in Part II, and who contributed much to the work in Part III,

Dr. Harris Notarys, who is my living encyclopedia of low temperature experimental techniques and from whom I have learned the "can-do" attitude,

John Gatewood, who has helped me in the reassembly of the JPL He^3 refrigerator and in numerous occasions thereafter. His cool efficiency still fills me with admiration,

Sandy Santantonio, who has fabricated with skillful craftmanship the superfluid needle valves and the cell for the flowing film experiment. My machining skills matured under his meticulous standards,

Mr. Trent Wells of the Trentwells Co., who kindly donated his service of grinding the cell for my super-thick film experiment,

Mr. Kenneth Evans of the Jet Propulsion Laboratory, for kindly taking the SEM pictures of the super-thick film cell surface,

Mr. Lee Brubaker of the Jet Propulsion Laboratory, for kindly taking precise measurements of the dimensions of the super-thick film cell,

Fellow graduate students Jeff Greif, Peter Taborek and Jeff Hamilton for many helpful conversations and suggestions,

And finally, to the Low Temperature Physics Group at Caltech, in whose environment I have learned to become an experimentalist and where I have learned that limited resources is no limitation to research.

The research in this thesis was supported in part by the National Science Foundation and by the Caltech-JPL President's Fund.

ABSTRACT

In Part I, we investigate the problem of the thickness of a flowing helium film. Past experiments have either confirmed Kontorovich's prediction that the flowing film is thinner than the stationary film, or have observed no difference (e.g. the experiment by Keller (6)). Goodstein and Saffman have proposed a theory that tries to reconcile the difference in observations as the result of slightly different experimental conditions between different experiments. Our experiment tried to test Goodstein-Saffman's theory by attempting to produce both thick and thinned flowing films in the same experimental setup but under slightly different conditions. We constructed a cell in which the temperature could be varied from about $0.5^{o}K$ to $1.9^{o}K$ and film thickness was measured by the capacitance technique. Film flow from an external bath into a stainless steel beaker was terminated in two ways - either in a velocity step function or in an oscillation. The film thickness in the first case showed a sharp jump. In the second case, film thickness oscillated at twice the frequency of the bath level oscillation. The same behaviour was observed from $0.5^{o}K$ to $1.9^{o}K$. Our result therefore (i) does not confirm Keller's result, which motivated Goodstein-Saffman's theory, (ii) shows that for Goodstein-Saffman's theory to be correct, the τ_1 in their theory would have to be much longer than one hour. The conclusion is that it is unlikely for any more stable state than the thinned film to exist.

In Part II, we study the feasibility of verifying Lifshitz's theory of Van der Waals force by measuring the helium film thickness on a nickel surface form a height of about 1.5 mm to 0 mm. In this range, the retardation effect predicted by the theory would be more evident. The film

thickness was measured at about 0.6°K by the capacitance technique on a horizontal parallel plate capacitor about 1.5 mm above the bath level. The level was raised in a virtual manner by applying a dc bias across the capacitor. With a properly balanced cell, the virtual level could be changed in a continuous manner from about 1.5 mm to about 40 μm. Our measurement shows a film profile about 350 Å thicker than predicted by theory. We suggest that the discrepancy maybe ascribable to the roughness of the metallic surface, a quantitative description of which is lacking. In view of this, a quantitative test of Lifshitz's theory will have to wait until a smooth metallic surface can be produced in a well-controlled manner.

In Part III, we investigate theoretically the existence of instability of the helium film under a strong electric field. We found that such an instability does occur when the film thickness reaches about 4000 Å for our existing cell geometry. We offer experimental evidence that we may have observed such an instability.

TABLE OF CONTENTS

INTRODUCTION

Although the existence of the helium film was first conjectured in 1939 by Rollin(1), its nature remained a mystery for a long time due to its extremely small thickness and the attendant experimental difficulty in measuring it.

The existence of a mobile helium film was first conjectured to explain the anomalously high "evaporation" rate of liquid helium. The average film thickness was roughly measured by determining the volume of liquid required to cover a large area with film.(2) Later experiments deduced the average thickness by measuring the period of inverted U-tube oscillations of two helium baths connected by a film.(3) Microbalance technique was then introduced to weigh the film and determine its thickness.(4) The first good quantitative method that not only determined the average film thickness but also its variation with height above the bath was by optical ellipsometry.(5) The method was however not without its many difficulties and absolute determination of the film thickness by the method was judged to be only provisional. In 1970, Keller pioneered the capacitance technique which is capable of measuring the film thickness to within a few Å.(6) Basically, the capacitor plates form part of the walls standing in a helium bath. Before liquid helium is introduced into the bath, the bare capacitance is measured. After liquid helium is introduced, the capacitance changes due to the film on the capacitor plates. The capacitance is measured by a highly stable and accurate capacitance bridge which can measure down to 10^{-19}farad and is capable of absolute accuracy of 10 ppm and comparison accuracy of 0.01 ppm. Before Keller, the capacitance technique had already been tried, but the

capacitor was always part of an RF resonance circuit in which the change in capacitance caused a change in the resonance frequency which was then measured. Although the technique was capable of comparable accuracy to Keller's, it required great sophistication in instrumentation. The usefulness of Keller's technique, therefore, depends largely on the ready commercial availability of a highly accurate bridge. General Radio introduced such an instrument, the GR1616, in the late 60's. Since 1970, most experiments on the helium film use Keller's technique.

On the theoretical side, Schiff first suggested in 1941 that formation of a helium film on a wall may be due to the Van der Waals attraction between the helium atoms and the wall.(7) Lifshitz proposed a general theory of the Vander Waals attraction between macrosopic bodies in 1954.(8) Unlike all earlier theories of the helium film which were only capable of semi-quantitative predictions, Lifshitz's theory gives a precise prediction of the film thickness and its variation with height for all surfaces - metallic or dielectric. For some unknown reason, no attempt was made to test Lifshitz's theory in the helium film until 1972 when Anderson and Sabisky used a phonon resonance technique to measure "thin"helium film (from 0 to 250 Å) on a dielectric surface.(9) Their result gives good confirmation of Lifshitz's theory.

In this thesis, we use the capacitance technique to investigate two particular problems of the helium film. The first concerns whether the thickness of a flowing film is the same as that of a stationary film. The question arose in 1956 when Kontorovich first proposed that a flowing film should be thinner than a stationary film due to the Bernoulli effect.(10) However, Keller performed an experiment in 1970 using the capacitance

technique and found that the thickness remained the same. Since then experiments have been performed which either support Keller's result (11) or Kontorovich's theory (12). Goodstein and Saffman proposed a theory which tried to explain why apparently contradictory results could be observed under different experimental situations (13). Our experiment tries to (i) repeat Keller's result under similar experimental conditions, (ii) by appropriately changing the experimental conditions slightly, show that the film can indeed become thinner in the flowing state, thus demonstrating Goodstein and Saffman's theory that both thick and thin flowing films are possible, depending on experimental conditions. Our experiment, however, failed to reproduce Keller's result and we observed a thinned film under all conditions. It is therefore concluded that Goodstein and Saffman's theory is unnecessary to accommodate for differences between different experiments. This is presented in Part I of the thesis.

The second problem we try to address is the feasibility of testing Lifshitz's theory for helium film on a metallic surface in the thick film regime (thickness from 400 to 2000 Å) where "retardation" effects may be apparent. This is presented as Part II of the thesis. Our conclusion is that almost all experimental difficulties can be overcome. The only remaining limitation is the surface preparation of the metallic surface. A cleaved crystal surface is highly desirable, if not necessary. Whereas the cleaved crystal surface is possible for Anderson and Sabisky's experiment on a dielectric surface(9), it certainly does not exist for a metallic surface. Our investigation shows what kind of surface smoothness will be required to demonstrate Lifshitz theory for the metallic surface.

Part III of the thesis is an outgrowth of Part II. During our

investigation of Part II, we naturally come to consider if the helium film remains stable under a strong electric field. We found that the film becomes unstable when the electric field exceeds a certain critical value. We present evidence that we may have observed this electrohydrodynamic instability.

As all the measurements are performed by the capacitance bridge, we will briefly explain its operation here. The bridge is an inductance ratio arm bridge in which two arms form part of the secondary coil in a toroidal core transformer (fig. 1). The ratio of the voltages in the two arms is highly invariant. Changes of permeability of the transformer core with age, humidity etc. have little effect on the ratio. We measure the capacitance of the unknown capacitor C_x by what is known as the 3-terminal method. This simply means that the unknown capacitor and all cables connecting it to the bridge are shielded by grounded cable or enclosure. At first sight, it may seem that capacitance between the high plate of C_x with the enclosure together with the capacitance between the low plate of C_x and the enclosure will form a capacitor in parallel with C_x itself. If this were the case, our apparent reading will be larger than the true value for C_x. However, as maybe seen in fig. 1, the capacitance between the high plate and grounded enclosure (together with the capacitance of the lead wire and its grounded shield) can be represented by C_{hg}. This leakage capacitance only serves to increase the load to the transformer ratio arms and does not affect the balance. Similarly, the leakage capacitance between the low plate and the grounded enclosure is represented by C_{lg}. This only reduces the sensitivity of the detector and again does not affect balance of the bridge. The 3-terminal method thus measures the

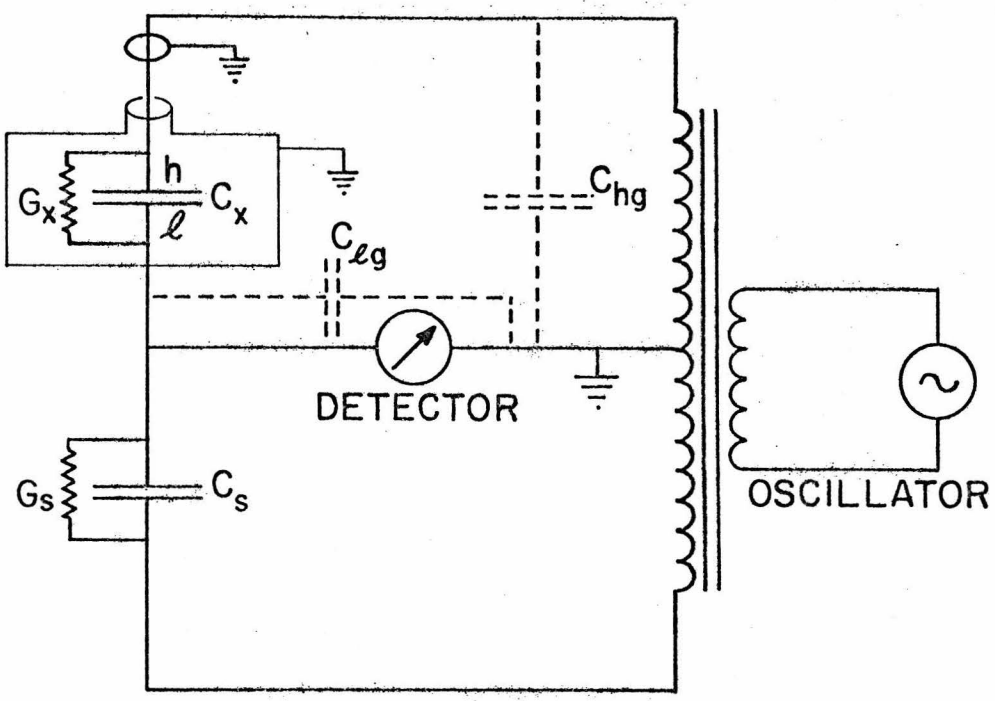

Fig. 1 Schematic diagram of the GR1616 capacitance bridge. C_x, G_x are the capacitance and leakage conductance of the unknown capacitor. C_s, G_s are the standard capacitor and resistor inside the bridge. C_{hg}, C_{lg} are the equivalent leakage capacitance from the high plate and low plate to ground. The diagram shows the unknown capacitor being measured by the "3-terminal" method.

true capacitance value. The bridge also separately balances the leakage conductance G_x across the unknown capacitor. For this purpose, the detector is a phase-sensitive detector with separate quadrature and in-phase meters.

All the experiments were carried out in a He^3 refrigerator at the Jet Propulsion Laboratory. With the He^3 refrigerator, it is possible to have temperature below 0.8°K so that there is practically no vapor between the capacitor plates to contribute to the capacitance. The refrigerator is capable of about 0.5°K for more than eight hours, more than adequate for our purpose. A schematic diagram of the refrigerator is shown in fig. 2. Detailed experimental methods will be separately discussed in Part I and Part II.

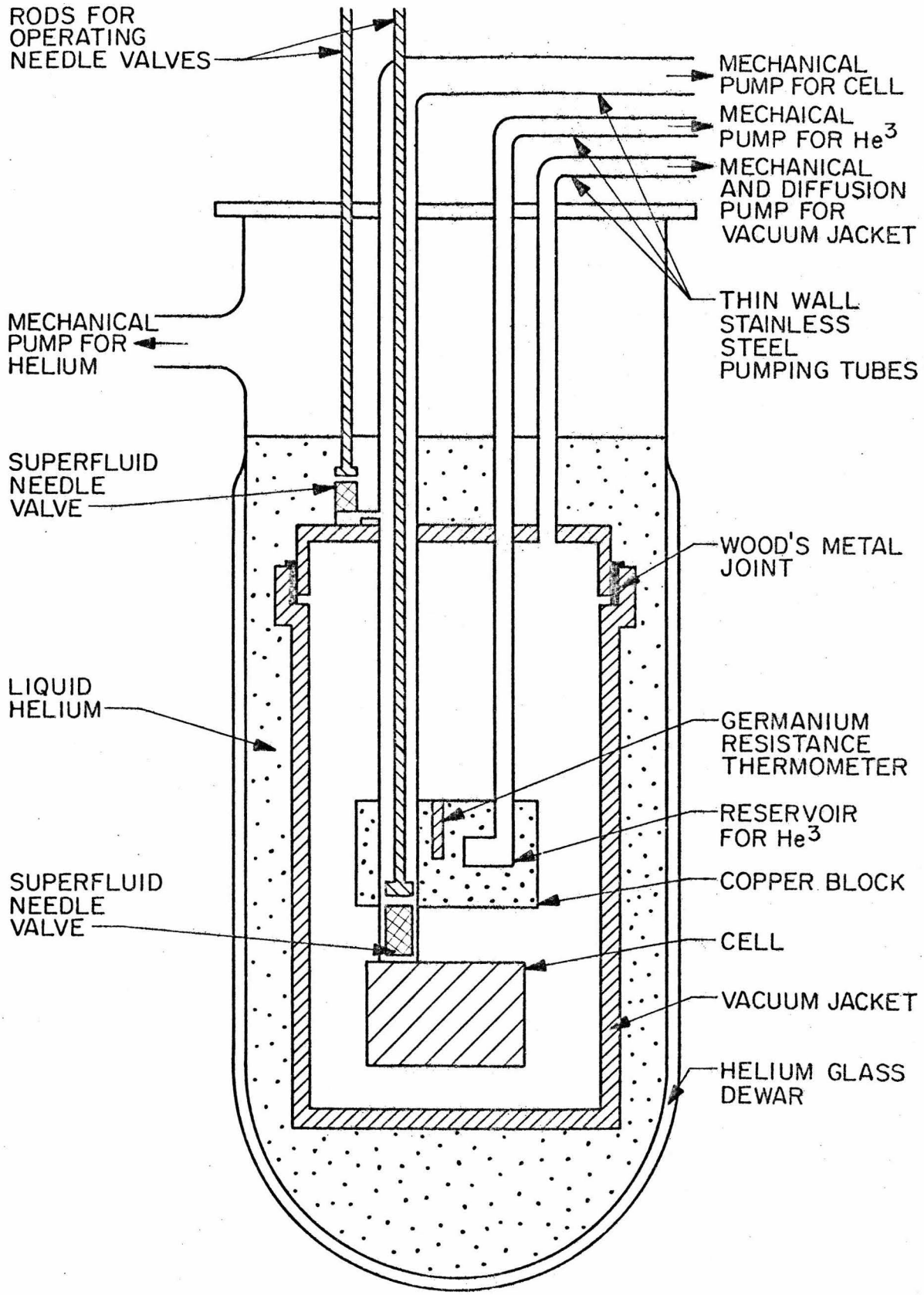

Fig. 2 Schematic diagram of the He^3 refrigerator.

PART I AN ATTEMPT TO PRODUCE BOTH THICK AND THINNED FLOWING SUPERFLUID FILMS †

I.1 INTRODUCTION

It has long been known that helium not only can form a film on a vertical wall but the film will also creep over the wall if the liquid level inside is higher than that outside. In 1941, Schiff suggested that the formation of the film is due to the Van der Waals force of the wall(7). The flowing of the film on a wall is then nothing more than potential flow of a nonviscous fluid under the combined action of the gravitational field and the Van der Waals force. Since then, research on the thick helium film (as distinct from films which are a few atomic layers thick) has centered around its flow rate, critical velocity, dissipation and third sound, which is a surface wave on the film.

In 1956, Kontorovich suggested that a flowing film should be thinner than a stationary film. This is a consequence of the Bernoulli equation from which we expect the pressure to be reduced when a liquid starts flowing. For a helium film, reduction in pressure can be achieved by a reduction in the film thickness, and hence the prediction. Keller tested the Kontorovich prediction in 1970 (6) and reported that the flowing film did not increase in thickness when the flow stopped. Later experiments by other investigators have either confirmed Keller's findings or have gotten exactly opposite results, i.e. confirming Kontorovich's prediction. In the confusion, there was serious speculation on the validity of the two-fluid model hydrodynamics for the helium film. Explanations were also put forth to either support or disprove Kontorovich's prediction.

† Published in J. of Low Temp. Phys., 27, 187 (1977)

Goodstein and Saffman (13) (14) later developed a theory trying to explain why apparently contradictory experimental results were obtained by different groups. Their theory predicts that the helium film will thin or remain thick under different experimental conditions. To test the Goodstein-Saffman theory, we have designed an experiment trying to produce both thick and thinned films under slightly different conditions but using the same experimental setup. The result however turned out to support Kontorovich's prediction in all cases. Goodstein-Saffman's theory, which has been put forth to accomodate different results, is therefore shown to be unnecessary. However, there still remains the mystery of why thick films have occasionally been observed by other investigators.

I.2 THEORY

Let us first consider the case of a static helium film on a vertical wall above a helium bath which is in equilibrium with its saturated vapor. The situation is depicted in fig.3. The external potential per unit mass for both vapor and liquid in the film and the bath is given by

$$\chi(y,z) = gz - \frac{\alpha}{y^3}$$

where g = acceleration due to gravity and where we have assumed the Van der Waals potential per unit mass due to the wall is given by $\frac{-\alpha}{y^3}$ for simplicity. The vapor in equilibrium is governed by

$$\nabla p(y,z) + \rho_v(y,z)\,\nabla\chi = 0$$

where p = pressure and ρ_v = density of vapor.

Assuming the ideal gas equation of state,

$$p(y,z) = \rho_v(y,z)\frac{kT}{m}$$

where m = mass of a helium atom, k =Boltzmann's constant and T = temperature

Hence $$\frac{\nabla p}{p} = -\frac{m\nabla\chi}{kT}$$

$$p(y,z) = p_0 \exp\left(\frac{-m\chi(y,z)}{kT}\right)$$

$$p_0 = p(\chi=0)$$

Since $\chi=0$ at $y=\infty$, $z=0$

Hence $$p_0 = p(y=\infty,z=0) = p_{sv} \equiv \text{saturated vapor pressure}$$

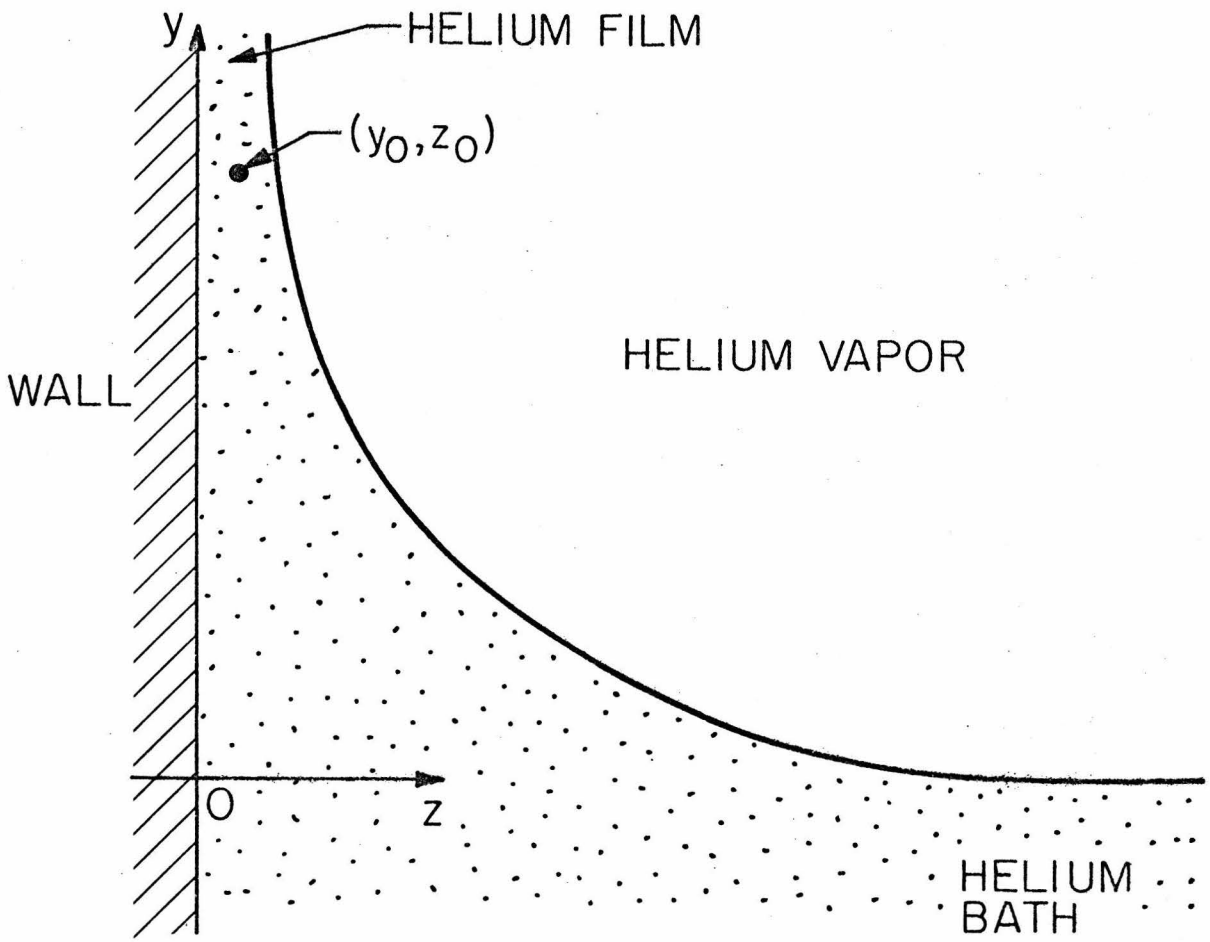

Fig. 3 Helium film on a vertical wall.

Therefore $$p(y,z) = p_{sv} \exp\left(\frac{-m\chi(y,z)}{kT}\right)$$

Now the vapor condenses whenever $p(y,z) > p_{sv}$. Hence the vapor phase exists where $\chi(y,z) > 0$ and liquid phase (film and bath) exists where $\chi(y,z) < 0$. $\chi = 0$ is therefore the liquid - gas interface and determines the film profile.

$$gz - \frac{\alpha}{y^3} = 0$$

$$y = \frac{\left(\frac{\alpha}{g}\right)^{1/3}}{z^{1/3}}$$

We have shown that the film profile is an isobaric surface for the gas.

Consider the problem from the liquid side. From the two-fluid model, the equation for the superfluid component is given by

$$\frac{\partial v_s}{\partial t} + \nabla\left(\frac{v_s^2}{2} + \tilde{\mu} + \chi\right) = 0$$

where $\tilde{\mu} = \mu(p,T) - \frac{1}{2}\frac{\rho_n}{\rho} v_s^2$

and $\mu(p,T)$ = chemical potential /unit mass for superfluid at rest

v_s = superfluid velocity

ρ_n = normal fluid density

ρ = density of liquid helium

First consider the static film. The equation becomes

$$\mu(p,T) + \chi = \text{constant} \qquad (1)$$

At the gas-liquid interface, $p = p_{sv} = \text{constant}$. Assuming T is also constant, μ will be constant, implying $\chi = \text{constant} = \chi(y=\infty, z=0) = 0$

We have shown again that $\chi = 0$ gives the static film profile. Now consider the case of steady flow where $\partial/\partial t = 0$

$$\frac{v_s^2}{2} + \tilde{\mu} + \chi = \text{constant throughout the liquid}$$

$$\mu + \frac{1}{2}\frac{\rho_s}{\rho} v_s^2 + \chi = \text{constant} \qquad (2)$$

We can find the constants in equation (1) and equation (2) by evaluating both eq.(1) and eq.(2) at $(y=\infty, z=0)$, i.e. the liquid-gas interface of the bath. Since $\chi = 0$ and $v_s = 0$ at $(y=\infty, z=0)$, it is easily seen that both constants in eq.(1) and eq.(2) are equal to $\mu(p_{sv},T)$.

Now consider a point (y_o, z_o) in the film which is below the film surface for both static and steady-flowing film (see fig. 3). Evaluating eq.(1) and eq.(2) at (y_o, z_o) and subtracting eq.(1) from eq.(2), we have

$$\mu_s(p,T) - \mu_f(p,T) = \frac{1}{2}\frac{\rho_s}{\rho} v_s^2$$

where μ_f = chemical potential for flowing film at (y_o, z_o)

μ_s = chemical potential for static film at (y_o, z_o)

Now from thermodynamics, we have

$$\Delta\mu = \frac{1}{\rho}\Delta p - s\Delta T$$

Assuming isothermal flow, $\Delta T = 0$

Hence $$p_s(y_o,z_o) - p_f(y_o,z_o) = \frac{1}{2}\rho_s v_s^2 \qquad (3)$$

where p_s = pressure for stationary film at (y_o,z_o)

p_f = pressure for flowing film at (y_o,z_o)

Thus the pressure at (y_o,z_o) will decrease by an amount = $\frac{1}{2}\rho_s v_s^2$ when the film starts flowing. This decrease in pressure can be achieved by a reduction in film thickness, i.e. by reducing the "hydrostatic head" over the point (y_o,z_o).

$$p_s - p_f = \rho\left(\frac{\alpha}{d_s^3} - \frac{\alpha}{d_f^3}\right)$$

where d_s = static film thickness and d_f = flowing film thickness. For small v_s and hence small change in d,

$$p_s - p_f = -3\rho\alpha\,\frac{\Delta d}{d^4}$$

where Δd = change in film thickness. Putting the expression into eq.(3) and defining $Q \equiv \rho_s v_s d/\rho$ (the volume flow rate per unit length of perimeter over the wall), we have

$$\Delta d = -\frac{1}{3}\left(\frac{\rho}{2\rho_s}\right)\frac{Q^2 d^2}{\alpha}$$

$$= -\frac{1}{3}\left(\frac{\rho}{2\rho_s}\right)\frac{Q^2}{gzd} \qquad (4)$$

e.g. for $\rho_s \simeq \rho$, z = 1 cm, d $\simeq$ 300 Å, Q $\simeq 10^{-4}$ c.c./cm.sec. (all these are typical measured values), $\Delta d \simeq -50$ Å, which should be a measurable quantity.

Keller performed an experiment in 1970 trying to observe this thinning of the flowing film. He found that for both outflow and inflow into a stainless steel beaker, the film thickness did not increase after the flowing had stopped.

Various explanations were offered to explain this. Looking at eq.(2), we see that when v_s changes from zero to a non-zero value, μ has to change to compensate. Now μ is a function of p and T. We have assumed T constant before so that for μ to change, p has to vary. The alternate explanation was that T may have changed so that p may remain constant, i.e. film thickness remains constant. This is in effect invoking the "fountain effect". However, later experiments show that the film flow is to a high degree of accuracy isothermal so that the alternate explanation is invalid.

Another explanation is that at the film interface, $\rho_s \to 0$ so that in eq.(2), although v_s may become greater than zero, the term $\rho_s v_s^2/\rho$ remains equal to zero. However, eq.(2) is valid throughout the thickness of the film, not just the surface. v_s, ρ_s are non-zero everywhere except near the surface. That the explanation is fallacious is quite obvious.

Goodstein and Saffman first tried to explain Keller's result by noting that if the film does decrease in thickness when it starts to flow, the new film-vapor interface will have $\chi < 0$ and the vapor pressure at the new interface will be greater than p_{sv}, i.e. the space vacated by the decrease in film thickness will be filled with supersaturated vapor. The supersaturated vapor will tend to condense and restore the film thickness. If the film thickness is restored to the previous saturated vapor isobar, we must however find an alternate source for the change in pressure

(to account for the change in μ which compensates the $\rho_s v_s^2/2\rho$ term in eq.(2)). Goodstein and Saffman suggested that surface tension forces will maintain a pressure difference across the interface so that pressure on the vapor side will be lower. This is analogous to the fact that a curved surface will support a pressure difference across the interface. In that case, a virtual displacement of the surface changes the surface area so that total surface energy is changed. This represents a force on the surface, i.e. under a virtual displacement δx of the surface, surface energy changes by $\delta E = \delta(\sigma.s) = \sigma\delta s$, where σ = surface tension coefficient, s = surface area. For curved surface, $\delta s \neq 0$. Thus $\delta E \neq 0$ for $\delta x \neq 0$. Thus $\delta E/\delta x \neq 0$, implying there is a force on the surface. For our case, the surface is plane and not curved. Goodstein and Saffman suggested that under δx, $\delta E = \delta(\sigma.s) = (\delta\sigma).s$, i.e. the surface tension coefficient changes with x rather than the surface area changes with δx. The net effect is the same - there is a net force on the surface which will act to support a pressure difference across the surface.

After Keller's experiment, there were quite a number of other investigators trying to reproduce his result. Some were in agreement but some found a decrease in film thickness as predicted by Kontorovich. The most notable of these are the experiments by van Spronsen et al (15) and by Packard and Williams(16). Van Spronsen et al used a glass capillary 166 m long and 0.35 mm i.d. to connect two helium baths. They found that when the film in the capillary was set into motion, the total amount of liquid in the two baths was observed to increase, from which they deduced that the film must have thinned. Packard and Williams observed the U-tube oscillation of two baths separated by a wall and

connected by the helium film running back and forth on the wall. They found that the film thickness oscillated at a frequency twice that of the bath levels. Since the bath levels "drive" the film, the film velocity also oscillates at the same frequency as the bath level. The film thickness will oscillate at twice the frequency as the velocity as Kontorovich's theory predicts that $d \propto v_s^2$. Packard and Williams' result is therefore a confirmation of Kontorovich's theory.

Goodstein and Saffman modified their theory to try to explain why thinning of the film can be observed at times. They noted that a thinned film requires time to recover its original thickness. This time θ depends on three different time constants - τ_1, the time for the film-vapor interface to restructure itself to be able to support the pressure difference; τ_2, the time for vapor to come from around the bath to replenish the region where condensation has occurred, and τ_3, the time for condensation to occur. In their theory, under certain approximations,

$$\theta = \frac{\tau_1 \tau_2}{\tau_3} \tag{5}$$

τ_1 is an unknown intrinsic time and

$$\frac{\tau_2}{\tau_3} = \left(\frac{5}{6\pi} \right)^{1/2} \left(\frac{\eta L^2}{\rho_v c_v r^3} \right) \tag{6}$$

where η, ρ_v and c_v are respectively the shear viscosity, density and sound speed of the vapor in contact with the film, and L and r are distances characteristic of the geometry of the apparatus. They then showed that in all of the experiments reporting thick films, $\tau_2/\tau_3 \simeq 1$, whereas in all the experiments reporting thin films, $\tau_2/\tau_3 \gg 1$, so that the

thinned state could be expected to persist for longer than the experimental observation time.

In order to test these ideas, we have constructed an apparatus designed to observe both regimes. In particular, we have taken care to follow the details of Keller's original cell to see whether that thick film result was reproducible. In the same apparatus, we can lower the temperature, changing ρ_v in eq. (6) sufficiently to increase τ_2/τ_3 by a number of orders of magnitude. The experiment then repeats the one by Williams and Packard which gave the thinned film result. In addition, the cell is designed so that the film flow can be terminated either in a velocity step function (for which case the Goodstein-Saffman equations are most easily solved) or in U-tube oscillations. If Kontorovich's prediction is correct, the velocity step should produce a sharp jump in film thickness whereas the U-tube oscillations should produce film thickness oscillations at twice the frequency.

I.3 METHOD

The cell we have constructed is essentially similar to Keller's. (fig. 4) The cell consists of a stainless steel "beaker" A seated in a well. Inside the beaker is a central post B to which a thin sleeve C is attached. Liquid helium is introduced via a superfluid needle valve to the reservoir, D, outside the beaker. The space between C and A is slowly filled up by film flow. The small gap between B and A forms the film thickness measuring capacitor while the capacitance between C and A measures the level of liquid helium inside the beaker.

The body of the cell, together with A, B, and C, are all made of 304 stainless steel. D has an o.d. of 3.77 cm at the reservoir level. A has an o.d. of 2.50 cm and i.d. of 2.25 cm. The beaker rim of A stands at a height of 2.62 cm above the lowest point in the outer reservoir. At the small gap between B and A, B has an o.d. of 2.235 cm and length 0.38 cm. Thus the film measuring capacitor is a coaxial capacitor of nominal gap width 76 μm and length 0.38 cm. C has an o.d. of 1.64 cm and length 5.84 cm. The top of B is 0.28 cm below that of A so that we are measuring film thickness at a distance of about 0.47 cm below the inner rim of the beaker. This is to ensure that we are measuring film thickness in a dissipation-free region of potential flow. All surfaces were finely machined and highly polished with grit 900 aluminum oxide. (This surface preparation procedure is the same as Keller's.) They were then washed in a solution of alconox, then acetone and finally in an ultrasonic bath of distilled water. All the electrodes A, B, C were insulated from each other by 0.13 cm thick spacers of bakelite. The various pieces were cemented together by epoxy (Stycast 2850 GT, catalyst 9)

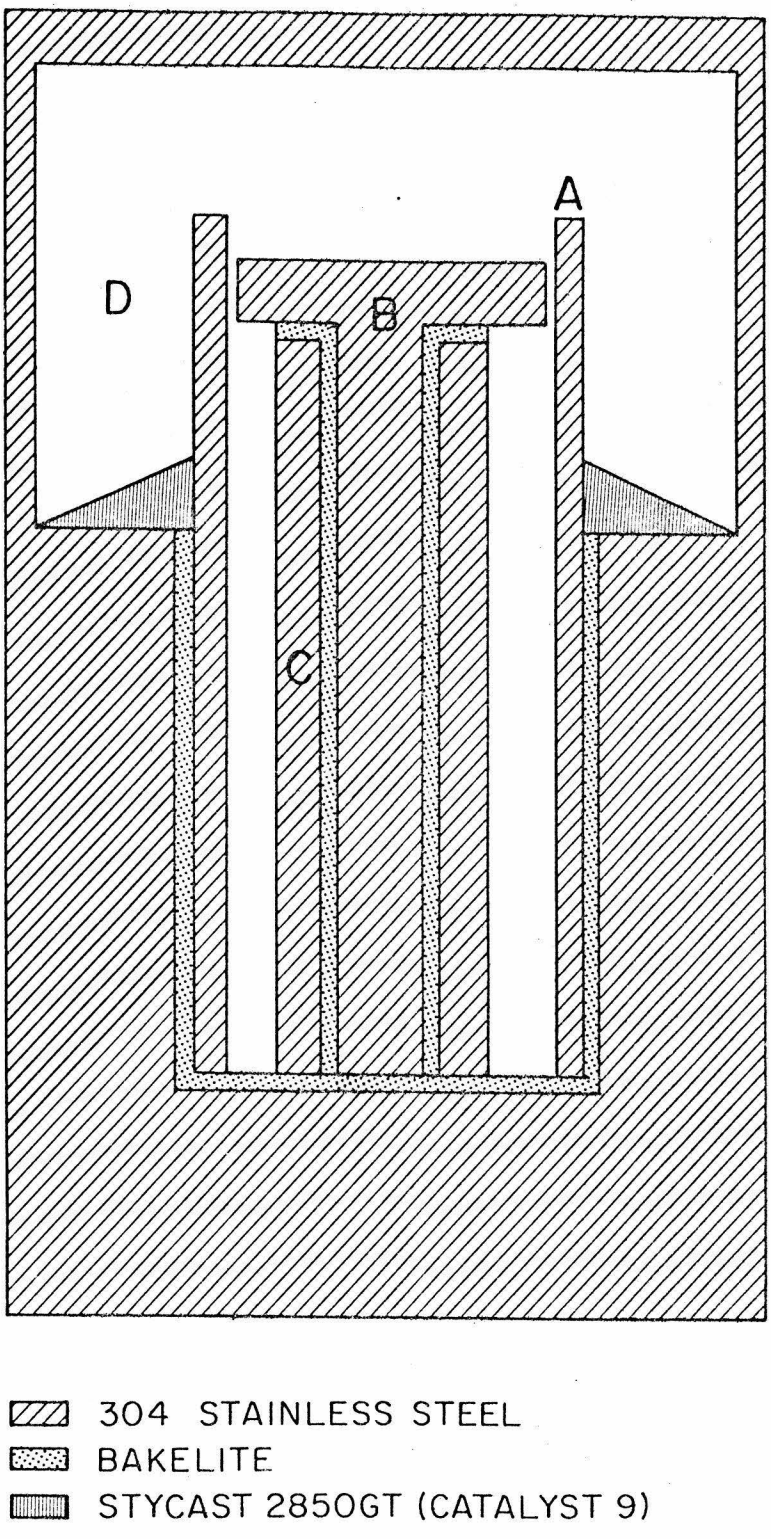

Fig. 4 Cross-sectional view of cell for flowing film experiment.

cured at room temperature. Following Keller, we at first tried epoxy Eccobond 26 and found it deficient in two aspects. Superfluid leaks developed through the epoxy after only a few runs at helium temperature. Furthermore, the mechanical strength of the epoxy left something to be desired. After several runs, the post began to vibrate so much that measurement of the film thickness became impossible. By contrast, Stycast 2850GT has much better mechanical strength and can easily be made superleak tight. There was one drawback to the use of Stycast 2850GT. On cooling down the cell, the epoxy went through a thermal history in which it "buckled" in discrete steps. On hindsight, this probably was due to the fact that curing was done at room temperature rather than at elevated temperature. As a result, the film thickness capacitor AB changed its gap width uncontrollably. The steps were usually quite small. In terms of eqivalent film thickness, they were usually about tens of angstroms in size (so that the real motion was fractions of angstroms). They occurred most frequently at the beginning of a run and their frequency decreased appreciably after the dewar had been kept cold for a few days. Although, as we shall see, we can unambiguously identify the steps due to epoxy buckling, the buckling made it impossible to measure the absolute film thickness directly. To rectify this situation, we can deduce the absolute film thickness from the period of the U-tube oscillations that occurred at the end of selected runs.

The cell after fabrication was attached to the He^3 refrigerator. Care was taken that during this process, no soldering flux or vapor could get into the cell. The cell was pumped for a few days with a mechanical pump with the help of a liquid nitrogen cold trap. It was also flushed

several times with helium gas before we began the runs. In between runs, the cell was always kept at high vacuum to prevent surface contamination.

At the beginning of each run a certain fixed amount of liquid helium was introduced via the superfluid valves from the outside bath into the reservoir outside beaker A. (see fig. 2 and 4) The film would then flow into the beaker over the surface of A. We note that in contrast to Keller's experiment where the flow surface is interrupted by regions other than stainless steel, our flow surface is an uninterrupted piece of stainless steel.

We made two types of runs depending on the amount of liquid helium initially in the reservoir and beaker. The first type was when we introduced sufficiently little helium into the reservoir that all of it emptied into the beaker. The end of the run was marked by a sudden depletion of liquid on the outside and consequently a step function in the velocity of the film. The second type involved starting with enough liquid in the reservoir so that the final level of equlibration between the inside and outside of the beaker was above the bottom of the reservoir. In this case, U-tube oscillation between the inside and outside levels occurred and the velocity of the film oscillated more or less sinusoidally. Usually we started with a run of the first type and monitored the film thickness at the end of the run. We then opened the superfluid valves letting more liquid into the reservoir. The end of the run was again monitored. By filling the reservoir repeatedly, we soon graduated from runs of the first type to runs of the second type. In between monitoring the film capacitor AB, we monitored the level capacitor AC, which gave information about flow-rate and liquid level at equilibrium. As we had only one capacitance

bridge, we could only monitor either AB or AC at one time. Knowing the flow rate and the final level of equilibrium allowed us to pinpoint the end of a run to within half a minute or even a few seconds. The film thickness change during this interval can only be attributed to the velocity variation at the end of the run. We used a time constant of 1 sec. in the capacitance bridge. The best resolution we got was about 0.5 Å of film thickness. The limiting factor seemed to be mechanical noise in the system. Stability of the bridge was better than 10^{-5} pf/hour. The bare capacitances of AB and AC were obtained by filling the beaker completely with liquid helium and measuring the change in capacitances. After lead capacitances were taken account of, we found AB to have 37.47 pf and AC to have 9.64 pf. AB is seen to have a greater value than the numerical calculated value of a coaxial capacitor. We ascribe this to edge effect and the central post being slightly off center. Adjustments were made in calibrations for the film thickness. Temperature was monitored by a germanium thermometer. Runs were made around three temperatures: between 0.5 - 0.7 °K, 1.4 - 1.5 °K and around 1.9 °K. Runs in the lower two temperature ranges could be maintained at a temperature stability of 1 m°K/hr. At 1.9 °K, it was more difficult to maintain temperature stability, but we found that even moderate temperature drift did not affect our results at all.

I.4 RESULTS

We will first discuss runs around 1.4 °K. The flow rate Q (in vol. of liquid/unit time/unit length of perimeter) in each run could be determined easily by measuring the rate of liquid level rise in the beaker. At the beginning of each run, Q was usually as high as 13.0×10^{-5} c.c./cm. sec. After the inside level has risen by about 1 cm, Q levelled off to about 11.2×10^{-5} c.c./cm sec. This value had a range of about $\pm 0.5 \times 10^{-5}$ c.c/cm sec. from run to run.

The liquid level in the beaker was monitored at the end of a typical type I run, i.e., a run in which all liquid helium from the reservoir has drained into the beaker (fig. 5(a)). The run was made at T = 1.34 °K and final equilibrium level Z was at 3.3 cm below the film thickness capacitor. It can be seen that the level rises at a steady rate before leveling off quite sharply. Since the velocity in the film is proportional to the rate of rise of the level, we see that the velocity jumps from a finite value to zero in a step function. Fig. 5(b) shows the behavior of the film in another run under similar conditions (T = 1.44 °K, Z = 3.2 cm). We see a jump in thickness of about 50 Å. There are small ripples at the edge of the jump. These can be interpreted as follows. After draining all the outside liquid into the beaker, the film does not stop immediately, draining itself in the process. It recovers itself in the series of high frequency ripples. This behavior was present in all the type I runs. It is less obvious in runs at large Z where the jump in film thickness is smaller but cleaner. As we increase the liquid level inside the beaker, (i.e., decreasing Z since Z is the level between the mid-point of film capacitor AB and the level) the ripples increase in amplitude and period,

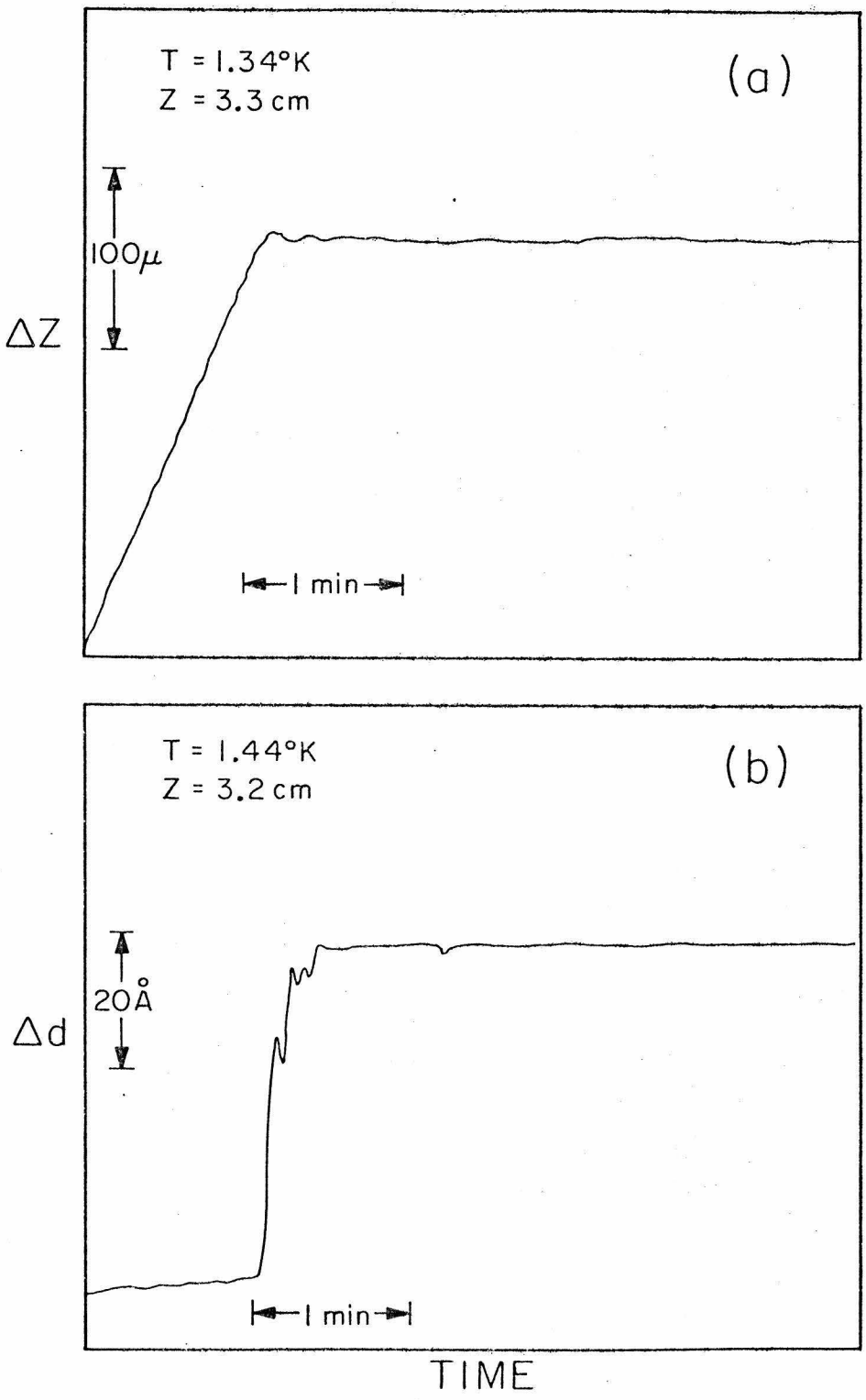

Fig. 5(a) Liquid level inside the beaker towards the end of a type I run.

(b) Film thickness towards the end of a type I run.

making a smooth transition to the behavior of type II runs (see below).

Fig. 6(a) shows the level in a typical type II run (T = 1.44 °K, Z = 1.90 cm). The U-tube oscillation of the level has an initial amplitude of about 55 μm and period of about 116 sec. The film thickness under similar conditions (T = 1.44 °K, Z = 2.02 cm) is shown in fig. 6(b). There is a sharp rise in film thickness of about 52 Å, followed by damped oscillations whose upper baseline remains at the peak level. (c.f. Williams and Packard (16), our trace in fig. 6(b) is just an inverted version of theirs.) We followed this final level for more than 80 minutes and the film thickness remained constant within ± 3 Å. The film oscillation has an average period of about 55.6 sec., which is slightly less than half the period of level oscillation (116 sec.). This difference can be adequately explained by the fact that the Z's are slightly different.

Below 1 °K, both type I and II behavior of the film were also observed. At 1.9 °K, we observed the same phenomena with the exception that film oscillation in type II runs were so heavily damped that only one to two cycles of the oscillations were apparent. Thus, qualitatively, we have confirmed Kontorovich's prediction from 0.5 °K to 1.9 °K with our cell geometry.

According to the Goodstein - Saffman theory, when a film is set suddenly in motion, it initially thins, then relaxes back to its unperturbed thickness with the time constant θ given in eqs. (5) and (6). Conversely, if a flowing film is brought suddenly to rest, as done in our experiment, the Goodstein - Saffman equations predict it will initially become thicker, then relax to its stable thickness with the same time constant. Thus, it is not the observation of a jump in film

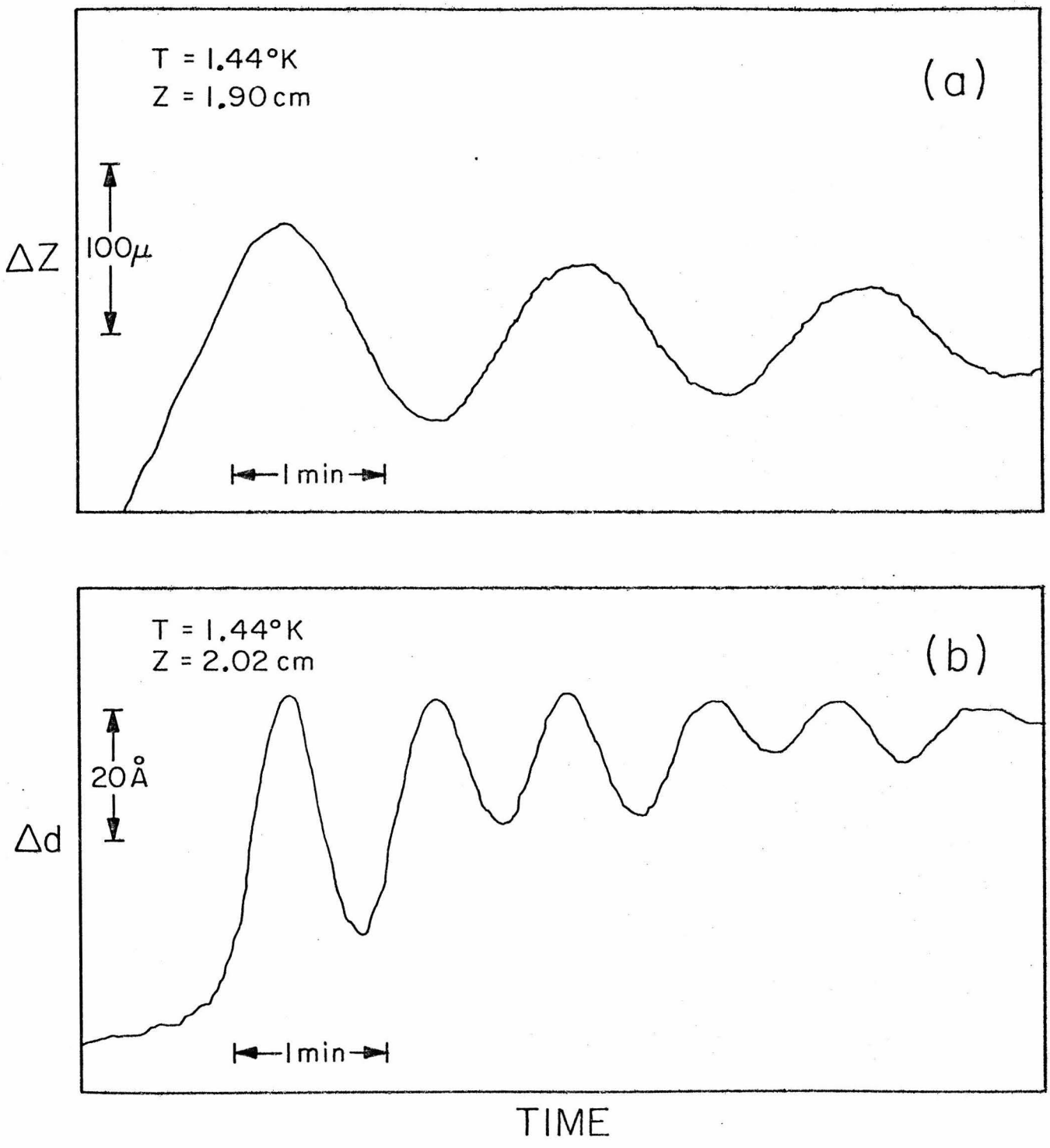

Fig. 6(a) Liquid level inside the beaker towards the end of a type II run.

(b) Film thickness towards the end of a type II run.

thickness upon termination of the flow, but rather the failure to relax subsequently that disproves the theory. Technically, these observations only serve to put a lower limit on τ_1: it must be large compared to approximately an hour to account for the observation. More important, however, the observations reported here at $T \simeq 1.4$ °K fail to reproduce the results reported by Keller, which motivated the theory in the first place. Thus although the theory cannot be proven wrong, it has been rendered unnecessary.

To get a more quantitative test of eq.(4), predicted by Kontorovich, we have to know the absolute film thickness as a function of height. As we mentioned, the absolute thickness could not be measured capacitively because the central post suffered micro-buckling due to the epoxy. Instead, we deduced the absolute film thickness from the frequency of the observed U-tube oscillations. According to Atkins(17), the period of U-tube oscillation is given by

$$\tau = 2\pi \left[\frac{\rho}{\rho_s} \frac{r}{g} \int_o^h \frac{dZ}{d(Z)} \right]^{1/2} \qquad (7)$$

where r is the radius of an open thin-walled beaker, d(Z) the thickness as a function of height and h the height of the beaker rim above the liquid level. This theory assumes that the outside reservoir has infinite area and neglects the very Kontorovich effect we are discussing here. If we assume the film thins when it starts to move and if the reservoir has a finite area, the correct formula is

$$\tau = 2\pi \left[\frac{\rho A}{\rho_s g} \int_1^2 \frac{dl}{d(l)p(l)} \right]^{1/2} \qquad (8)$$

where 1,2 are where the film enters the inside and outside bath levels and

where A is the reduced area of the reservoir and the liquid surface inside the beaker. (1/A = 1/reservoir area + 1/area of liquid in the beaker) d(l), p(l) are the thinned film thickness and perimeter at position l along the path between the reservoirs. We note that τ goes roughly as $A^{1/2}$. In our cell, the reservoir does not have a flat bottom, but rather one that is slanted (see fig.4). When the final liquid level equilibrates in the slanted position of the reservoir, the reduced area A changes rapidly with Z so that τ should also change rapidly with Z.

In fig.7, we have plotted $\tau(\rho_s/\rho)^{1/2}$ vs Z for runs at temperatures ranging from 0.6 °K to 1.9 °K. From eq.(8), Atkins' theory predicts that $\tau(\rho_s/\rho)^{1/2}$ should be roughly independent on temperature (except for the factor d(l) on the right hand side of eq.(8) which depends weakly on ρ_s/ρ when thinned). Indeed, we can see the experimental points from wide-ranging temperatures falling roughly on the same curve. The solid line in fig. 7 is a representation of the theory which we fitted self-consistently, using as a model of the static film

$$d = \frac{335 \times 10^{-8}}{z^{1/3}} \text{ cm} \qquad (9)$$

The sharp rise in τ predicted by theory in the range 1.73 cm < Z < 2.14 cm is followed nicely. For Z >2.14 cm, τ does not drop off to zero abruptly. This could be due to crevices in the bottom of the reservoir. It could also be due to the film going into self-draining oscillations after it has depleted the outside reservoir, as mentioned earlier.

The fit to theory shown in fig. 7 is not sensitive to the exponent of Z in eq.(9), but it is sensitive to the coefficient. Thus, we can say

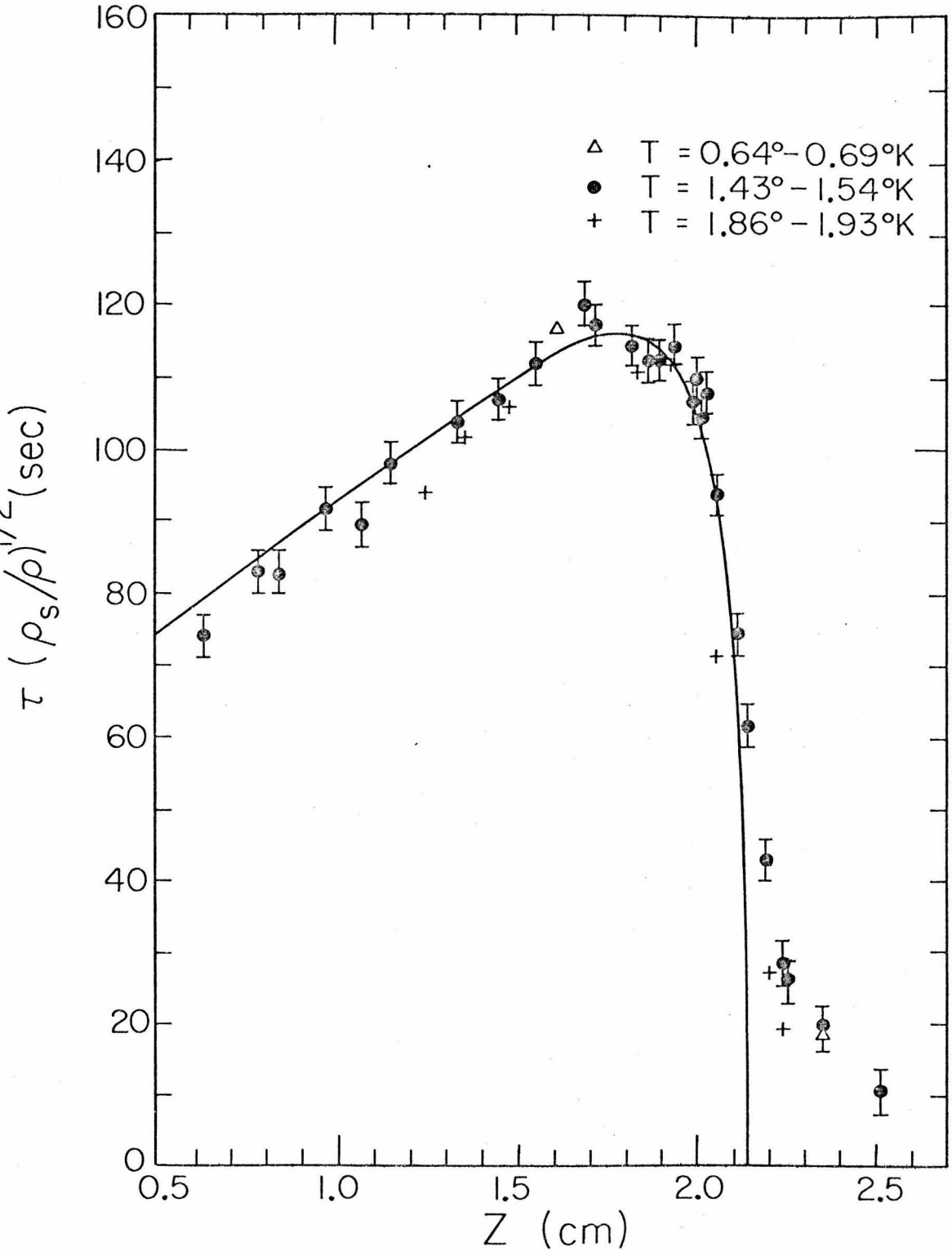

Fig. 7 $\tau(\rho_s/\rho)^{1/2}$ vs Z

that the film thickness at Z = 1 cm is d(1cm) = 335 ± 10 Å. We note that our absolute film thickness is much smaller than Keller's result of 460 - 480 Å at 1 cm. According to a theory of Lifshitz(8), and depending on the model of the dielectric functions used(9), the helium film thickness (at 1 cm) on metals should be between 240 Å and 290 Å with which our value compares more favorably. Using as a model of our film $d = 335 \times 10^{-8}/Z^{1/3}$ cm we can compare the Δd we have measured with Kontorovich's prediction.(eq.(4)) From run to run, Δd can differ quite appreciably. Δd observed/ Δd predicted ranges from about 0.85 to 1.35 at $T \simeq 0.6$ °K and $T \simeq 1.4$ °K. For $T \simeq 1.9$ °K, the ratio is more like 1.5. However, in each run, d's are quite consistent in that they follow the tendency of increasing with decreasing Z.

I.5 CONCLUSION

We have observed kinetic film thinning in the temperature range 0.5 °K to 1.9 °K, using a cell similar to Keller's. In response to a step function in the film velocity, the thickness jumps as predicted by Kontorovich. In response to oscillations in the film velocity, the thickness oscillates at twice the frequency, again as predicted by Kontorovich's theory. Quantitative agreement with the theory is only approximate for unknown reasons.

As Goodstein and Saffman have pointed out, the scientific question posed by the thickness of the flowing film is the following : if the film thins as predicted by Kontorovich, the space it vacates is filled with supersaturated vapor. This situation will not be stable if there exists some other state of the flowing film with lower free energy. There is no a priori way of knowing whether such a state exists, but Keller's result tended to indicate it did. Goodstein and Saffman then showed that whether that state was observed or not in a given experiment depended on the design of the experiment. The results presented here both cast doubt upon that original observation, and leave us without reason to believe that any more stable state than the thinned film exists.

PART II A STUDY OF THE FEASIBILITY OF VERIFYING LIFSHITZ'S THEORY OF VAN DER WAALS FORCE FOR A METALLIC SURFACE

II.1 INTRODUCTION

As is now well known, Van der Waals first attempted to improve the equation of state of a dilute gas by incorporating the effects of molecular interaction. The central idea is that gas molecules attract each other by a long range interaction, the nature of which was left unclarified.

In 1930, London showed that this interaction can be explained in terms of the spontaneous mutual polarization between neutral molecules.(18) In terms of the then just invented quantum mechanics, the interaction energy is given by the second order perturbation of the dipole-dipole interaction. (The case of hydrogen atom is shown in Ref. 28). This provides the now well-known result that inter-molecular attraction varies as $1/R^6$.

Schiff in 1941 (7) conjectured that the existence of the helium film on a wall may be due to the Van der Waals attraction between the helium atoms and the wall. His estimate of the film thickness agrees roughly with the measured value. The observed variation of film thickness with height above the bath level was known roughly to be $d \propto 1/Z^{1/3}$, where d is the film thickness and Z is the height above the bath level. This was also shown to be a consequence of the Van der Waals interaction. However, both theory and measurements were sufficiently crude at the time that neither could be used as a precise test nor prediction for the other.

Casimir and Polder showed in 1948 (19) that the application of

quantum electrodynamics again produces the $1/R^6$ interaction between atoms. However, as the separation between the atoms becomes greater than λ, where λ is the wavelength corresponding to the transitions between the ground state and excited states of the atom, then the interaction energy goes as $1/R^7$. Casimir and Polder ascribed this to the fact that retardation effects now become important. Although this sounds eminently reasonable, Casimir and Polder admitted that they could not find any classical or heuristic argument where retardation can be shown in a direct manner to produce the $1/R^7$ dependence.

In 1954, Lifshitz proposed a general theory of the Van der Waals force where the interaction between two macroscopic bodies is supposed to occur through the medium of the fluctuating electromagnetic field(8). This fluctuating field always exists in the interior of any absorbing medium, "and also extends beyond its boundaries - partially in the form of travelling waves radiated by the body, partially in the form of standing waves which are damped exponentially as we move away from the surface of the body." (8) The theory requires for its description only a detailed knowledge of the frequency-dependent dielectric susceptibilities of the bodies involved. It is supposed to be valid for any body whether it is magnetic, dielectric, or a conductor. It is also supposed to be valid for any temperature. The important point is that the frequency dependent dielectric susceptibility should in nature be measurable independently by spectroscopy. Dzyaloshinskii, Lifshitz and Pitaeviskii later grounded the theory in a more rigorous manner on quantum statistical mechanics(20). The essential features, however, remain the same. The authors worked out some simple limiting cases, including the case of the thickness of a

helium film on a wall. They showed that again $d \to a/Z^{1/3}$ for small d and for large thickness $d \to b/Z^{1/4}$, where a, b are constants calculable from a knowledge of the frequency-dependent dielectric suspectibility of the wall material and of helium.

Direct measurement of the Van der Waals force between two solid bodies was first attempted in 1954 for two flat plates of quartz separated by 1000 - 4000 Å.(21) Later efforts along this line produced results tending to confirm Lifshitz's theory in the retarded limit.(22)

A detailed confirmation of Lifshitz's theory has long been hindered by two facts: (i) the considerable experimental difficulty involved, (ii) the theory seems to require a detailed knowledge of the dielectric susceptibilities of the substances involved over the entire frequency range. Although spectroscopy provides this information for some substances over certain frequency ranges, it is not known how much the missing information will affect the prediction of the theory. Parsegian and Ninham (23) did a detailed analysis and found that careful modelling of the dielectric susceptibility with only a few terms will be sufficient for most substances to produce accurate predictions from the theory.

Anderson and Sabisky (9) in 1972 pioneered an ingenious approach to test Lifshitz theory in great detail. They measured the unsaturated film thickness of a helium film on the cleaved surface of single crystals of CaF_2, SrF_2 and BaF_2 doped with 0.02 mol% of the paramagnetic ion divalent thulium. The paramagnetic spins of the crystals are tuned by a magnetic field into resonance with some incident microwave radiation. The spins absorb the microwave and generate phonons. The phonons on hitting the cleaved surface of the crystal usually will reflect back.

However, if a helium film exists on the surface and has a thickness which is an odd multiple of $\lambda/4$, (where λ = acoustic phonon wavelength in helium) transmission of phonons through the surface will be enhanced with a subsequent lowering of the spin temperature which can be measured by optical dichroism. The film thickness can thus be measured accurately by counting the number of quarter wavelengths. The success of the technique hinges on the short wavelength of the acoustic phonons, in this case only about 40 Å, much smaller than the thickness of the helium film so that wavelength counting can be accurate. By the same token, the same technique will not work optically, which is the reason it has not been tried before. Anderson and Sabisky measured the unsaturated film from 10 Å to 250 Å as a function of the unsaturated vapor pressure. They also calculated Lifshitz's theory's prediction by modelling the dielectric functions of the crystals and helium in the manner as described by Parsegian and Ninham. The prediction is in excellent agreement with the measurements.

Our study tried to determine the feasibility of testing Lifshitz's theory in the regime not covered by Anderson and Sabisky's result. More specifically, we try to see:

(i) whether helium film thickness in the thick film limit can be measured so that the retardation effect as predicted by the theory can be more pronouncedly demonstrated. For helium film, this means a thickness greater than about 400 Å (corresponding to about 2.5 mm height above bath level). Measurement for film thickness much greater than 400 Å has never been seriously attempted.

(ii)whether film thickness can be measured accurately for a metallic surface where dielectric functions depends on a single parameter -

the plasma frequency of the metal. Because there is less uncertainty in modelling, comparison between measurement and prediction would be unambiguous.

II.2 NUMERICAL INTEGRATION OF THE LIFSHITZ FORMULA

In this section, we shall first discuss some of the qualitative features of the integral in the Lifshitz formula. Then we shall show the method of numerical integration and the computer program that carries out the integration. Finally, predictions for the helium film thickness on various metals will be computed. A simple interpolation formula will also be developed.

The Lifshitz theory calculates the interaction energy/unit area for a situation as shown in fig. 8.

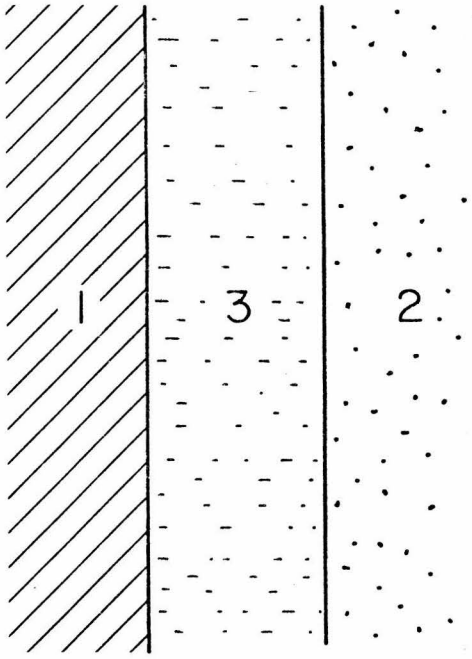

Fig. 8 Three macroscopic media with interfaces close to each other.

To calculate the thickness of helium film as a function of height above the bath level, we simply take medium 1 to be the wall, medium 2 to be the saturated helium vapor and medium 3 to be the helium film. The derivative of the interaction energy/unit area with respect to the thickness gives the energy/unit volume for liquid at the surface of the film. As we have shown in Part I, equating this energy in magnitude with the gravitational potential energy gives the thickness as a function of height. The explicit result is as follows:

$$Z(d) = \frac{V(d)}{\rho g} = \frac{\hbar}{2\pi^2 c^3 \rho g} \int_0^\infty \int_1^\infty p^2 \zeta^3 \varepsilon_3^{3/2} \left[\{ \frac{(s_1+p)(s_2+p)}{(s_1-p)(s_2-p)} \exp(\frac{2p\zeta d}{c}\sqrt{\varepsilon_3}) - 1 \}^{-1} \right.$$

$$\left. + \{ \frac{(s_1+p\varepsilon_1/\varepsilon_3)(s_2+p\varepsilon_2/\varepsilon_3)}{(s_1-p\varepsilon_1/\varepsilon_3)(s_2-p\varepsilon_2/\varepsilon_3)} \exp(\frac{2p\zeta d}{c}\sqrt{\varepsilon_3}) - 1 \}^{-1} \right] dp\, d\zeta$$

where $V(d)$ = Van der Waals energy/unit volume at the surface of a film with thickness d

$Z(d)$ = height as a function of film thickness

c = velocity of light

$2\pi\hbar$ = Planck's constant

$s_\alpha = (p^2 - 1 + \varepsilon_\alpha/\varepsilon_3)^{1/2}$ $\alpha = 1$ and 2

$\varepsilon_1, \varepsilon_2, \varepsilon_3$ = dielectric susceptibilities evaluated on the imaginary frequency axis at frequencies $\omega = i\zeta$. Subscripts 1, 2, 3 refer to the wall, helium vapor and helium film respectively.

Although the integral looks complicated, we can first deduce some qualitative features of it by examining the integrand. $Z(d)$ is a two-dimensional integral over the $p\zeta$ plane. Because of the exponential

factors, the integrand achieves its maximum value when $p \simeq \zeta_d/\zeta$ where $\zeta_d = c/2$. Hence for $\zeta = \zeta_d$, the maximum of the integrand occurs at $p = 1$. Besides ζ_d, there is another characteristic cut-off frequency in the integral - ζ_o. ζ_o is the frequency above which ε_1, ε_2, ε_3 all approach 1. Contributions to the integral from frequencies greater than ζ_o will be negligible.

There are now two regimes of approximation (see fig. 9):

(i) when $\zeta_d > \zeta_o$, i.e, small d (refer to the upper curve in fig. 9). In this case we consider the limits of integration to be from $p = 1$ to ∞ and $\zeta = 0$ to ζ_o. In this region, the maximum of the integrand occurs at $p >> 1$. Hence $s_1 \simeq s_2 \simeq p$. Using this approximation, Lifshitz showed that $V(d) \propto 1/d^3$.

(ii) when $\zeta_d << \zeta_o$, i.e. d large (refer to the lower curve in fig. 9). In this case, we can take $\varepsilon(\zeta) = \varepsilon(0)$. Lifshitz shows that this will imply $V(d) \propto 1/d^4$.

From both cases, we see that $\zeta > \zeta_d$ does not contribute much to the double integral because $\zeta > \zeta_d$ implies that at that particular ζ, integrand maximizes at $p < 1$. Since the integral over p is from 1 to ∞, $\int_1^\infty dp$ for that particular ζ will be small. This is true for all $\zeta > \zeta_d$. Thus ζ_d and ζ_o are two independent cut-off frequencies, the lower of which determines the effective cut-off frequency.

For numerical integration, we note that the integrand actually exponentially decays in both p and ζ and so we can apply Gauss-Laguerre quadrature along both p and ζ to find the integral. To see this more clearly, we have to transform variables.

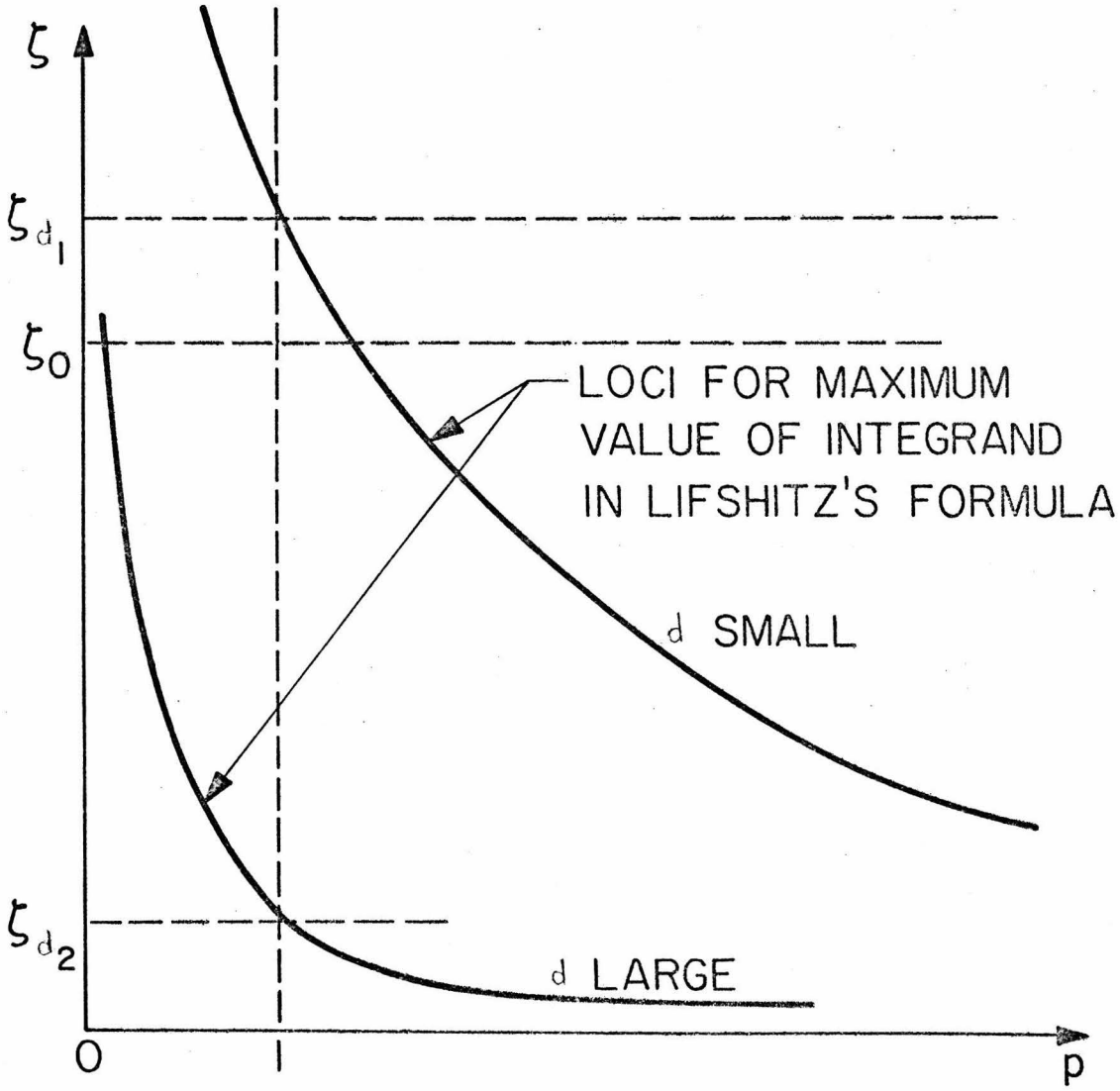

Fig. 9 Loci for maximum value of integrand in Lifshitz's formula in the $p\zeta$ plane.

First for fixed ζ, we work out the integral with respect to p. Let

$$f_1(p) = \frac{(s_1+p)(s_2+p)}{(s_1-p)(s_2-p)}$$

$$f_2(p) = \frac{(s_1+p\varepsilon_1/\varepsilon_3)(s_2+p\varepsilon_2/\varepsilon_3)}{(s_1-p\varepsilon_1/\varepsilon_3)(s_2-p\varepsilon_2/\varepsilon_3)}$$

Define integral over p

$$\equiv \int_1^\infty dp = \int_1^\infty p^2 \left\{ \frac{1}{f_1(p)\exp(2p\zeta d\sqrt{\varepsilon_3}/c) - 1} + \right.$$

$$\left. \frac{1}{f_2(p)\exp(2p\zeta d\sqrt{\varepsilon_3}/c) - 1} \right\} dp$$

let $\alpha = \dfrac{2\zeta d\sqrt{\varepsilon_3}}{c}$

$\beta = \dfrac{\alpha}{\sqrt{\varepsilon_3}}$

$q = \alpha p$

Then

$$\int_1^\infty dp = \frac{1}{\alpha^3} \int_\alpha^\infty q^2 dq \left(\frac{1}{f_1(\frac{q}{\alpha})e^q - 1} + \frac{1}{f_2(\frac{q}{\alpha})e^q - 1} \right)$$

Let $r = q - \alpha$

$$\int_1^\infty dp = \frac{1}{\alpha^3} \int_0^\infty (r+\alpha)^2 \, dr \left(\frac{1}{f_1(\frac{r}{\alpha}+1)e^{r+\alpha}-1} + \frac{1}{f_2(\frac{r}{\alpha}-1)e^{r+\alpha} - 1} \right)$$

$$= \frac{e^{-\alpha}}{\alpha^3} \int_0^\infty e^{-r}(r+\alpha)^2 \, dr \left(\frac{1}{f_1(\frac{r}{\alpha}+1)-e^{-(r+\alpha)}} + \frac{1}{f_2(\frac{r}{\alpha}+1)-e^{-(r+\alpha)}} \right)$$

$$= \frac{e^{-\alpha}}{\alpha^3} \int_0^\infty e^{-r} f(r)\, dr$$

where $f(r) = (r+\alpha)^2 \left(\frac{1}{f_1(\frac{r}{\alpha}+1) - e^{-(r+\alpha)}} + \frac{1}{f_2(\frac{r}{\alpha}+1) - e^{-(r+\alpha)}} \right)$

Let $$\int_0^\infty e^{-r} f(r)\, dr \equiv I(\zeta)$$

$I(\zeta)$ can be approximated by Gauss - Laguerre quadrature. If we choose a 15 - term approximation,

$$I(\zeta) \simeq \sum_1^{15} W(r_i)\, f(r_i)$$

where r_i = ith zero of the 15th order Laguerre polynomial

and $W(r_i)$= associated weight function

The values of the zero's and the associated weight functions can be found in Ref.(27). Once $I(\zeta)$ is known, we can integrate over ζ

$$\text{Integral over } \zeta \equiv \int_0^\infty d\zeta = \int_0^\infty \frac{\zeta^3 \varepsilon_3^{3/2} e^{\alpha}}{(\frac{2\zeta d}{c} \sqrt{\varepsilon_3})^3} I(\zeta)\, d\zeta$$

$$= \frac{c^3}{8d^3} \int_0^\infty e^{-\alpha} I(\zeta)\, d\zeta$$

Let $\beta = \frac{2\zeta d}{c}$

$$\int_0^\infty e^{-\alpha} I(\zeta)\, d\zeta = \int_0^\infty e^{-\beta}\, e^{\beta-\alpha}\, I(\zeta)\, d\zeta$$

$$= \frac{c}{2d} \int_0^\infty e^{-\beta}\, e^{\beta(1-\sqrt{\varepsilon_3})}\, I(\tfrac{c\beta}{2d})\, d\beta$$

Let $F(\beta) = e^{\beta(1-\sqrt{\varepsilon_3})}\, I(\frac{c\beta}{2d})$

$$Z(d) = \frac{\hbar}{2\pi^2 c^3 \rho g} \cdot \frac{c^3}{\delta d^3} \cdot \frac{c}{2d} \int_0^\infty e^{-\beta} F(\beta)\, d\beta$$

$$= \frac{\hbar c}{32\, ^2 d^4\, g} \sum_1^{15} W(\beta_i)\, F(\beta_i)$$

where again β_i, $F(\beta_i)$ are the zero's and associated weight functions of the 15th order Laguerre polynomial.

Before we can evaluate the integral, we have to put in the dielectric functions of helium and the metallic surface involved. For liquid helium, we use Anderson and Sabisky's model:

$$\varepsilon_3(\zeta) = 1 + \frac{0.016}{1+(\frac{\zeta}{\omega_1})^2} + \frac{0.036}{1+(\frac{\zeta}{\omega_2})^2} + \frac{0.0047}{1+(\frac{\zeta}{\omega_3})^2}$$

where $\omega_1 = 3.22 \times 10^{16}$

$\omega_2 = 3.74 \times 10^{16}$

$\omega_3 = 12.0 \times 10^{16}$

For helium gas, we take $\varepsilon_2(\zeta) = 1$

For the metal surface, ε depends only on the plasma frequency and comes in a simple form:

$$\varepsilon_1(\zeta) = 1 + \left(\frac{\omega_p}{\omega}\right)^2$$

where $\omega_p \equiv$ plasma frequency

$$= \left(\frac{4\pi N_o \rho e^2}{Am_e}\right)^{1/2} \quad \text{in c.g.s.}$$

where N_o = Avogadro's number

A = atomic weight of metal

ρ = density

m_e = mass of electron

The above formula of plasma frequency strictly speaking is only valid for noble metals. In general, plasma frequency can be determined experimentally by spectroscopy and usually lies in the range of 5 - 10 ev.

Using the Gauss - Laguerre quadrature and the dielectric functions, we have generated the following computer program that calculates Z(d) for any given plasma frequency.

```
C     GAUSS-LAGUERRE QUADRATURE OF LIFTSCHITZ FORMULA
      DOUBLE PRECISION BSUM,F1,F2,F(15),SUM,BIGF(15),X(15),
     1W(15), FREQ,E3,ALPHA,E1,P,S1,S2
      REAL D, WP, CONST, C, W1, W2, W3, Z
      DATA (X(I), I=1,15)/0.093307812017D0,0.492691740302D0,
     11.215595412071D0,2.269949526204D0,3.667622721751D0,
     25.425336627414D0,7.565916226613D0,10.1202856801900,
     313.130282482176D0,16.654407708330D0,20.776478899449D0,
     425.623894226729D0,31.407519169754D0,38.530683306486D0,
     548.026085572686D0/, (W(I),I=1,15)/2.18234885940D-1,
     63.42210177923D-1,2.630275779420-1,1.26425818106D-1,
     74.02068649210D-2,8.56387780361D-3,1.21243614721D-3,
     81.11674392344D-4,6.45992676202D-6,2.22631690710D-7,
     94.22743038498D-9,3.92189726704D-11,1.45651526407D-13,
     11.48302705111D-16,1.60059490621D-20/
      DATA C/2.997925E10/,W1,W2,W3/3.22E16,3.74E16,12.E16/

      ACCEPT 5, WP, I1,I2,I3
  5   FORMAT (E10.0,3I4)
      TYPE 7, WP
  7   FORMAT (20H1PLASMA FREQUENCY = , 1PE9.3//)
      DO 6 K=I1,I2,I3
      D=K*1.E-8
      CONST = (1.0545E-27*C)/(32.*3.1415926**2*D**4*0.1*5126*981.)
      BSUM=0.
      DO 10 I=1, 15
      FREQ = C*X(I)/(2.*D)
      E3 = 1. + 0.016/(1.+(FREQ/W1)**2) + 0.036/(1.+(FREQ/W2)**2)
     1+ 0.0047/(1.+(FREQ/W3)**2)
      ALPHA = X(I) * DSQRT(E3)
      E1 = 1. + (WP/FREQ)**2

      SUM =0.
      DO 20 J=1,15
      P=(X(J)/ALPHA)+1.
      S1 = DSQRT(P**2 -1.+(E1/E3))
      S2 = DSQRT(P**2 -1.+(1./E3))
      F1 = (S1+P)*(S2+P)/((S1-P)*(S2-P))
      F2 = (S1+P*E1/E3)*(S2+P/E3)/((S1-P*E1/E3)*(S2-P/E3))
      F(J)=(X(J)+ALPHA)**2*(1./(F1-DEXP(-X(J)-ALPHA))+1./(F2-
     1DEXP(-X(J)-ALPHA)))
 20   SUM=SUM+F(J)*W(J)
      BIGF(I)=SUM*DEXP(X(I)*(1.-DSQRT(E3)))
 10   BSUM=BSUM+BIGF(I)*W(I)
      Z=-CONST*BSUM
      D=D*1.E8
      ZD3=Z*D**3*1.E-7
      VD3=Z*981.*(4.004/6.02252E10)*D**3
  6   TYPE 50, Z, D, ZD3, VD3
 50   FORMAT(1PE10.3,10X,0PF5.0,10X,0PF6.3,10X,0PF6.3)
      STOP
      END
```

As an example, Z(d) for d from 250 Å to 2000 Å is calculated for nickel (ω_p = 10.0 ev or 8.3 ev, depending on different experiments). The results are tabulated in Table 1 and plotted on fig. 10. As can be seen from the figure, although the plasma frequency in not well determined for nickel, Z(d) is not very sensitive to its value.

As the computer program can only generate Z for discrete values of d, it would be useful to have an approximate interpolation formula. Since we know that Z(d) goes from $1/d^3$ to $1/d^4$ as d increases, we may write

$$Z(d) = \frac{\alpha_o}{\rho g d^3 (1+\frac{d}{d_o})} \tag{10}$$

or

$$\frac{1}{Zd^3} = (\frac{\rho g}{\alpha_o}) + (\frac{\rho g}{\alpha_o d_o})d$$

We plot the computer generated values of $1/Zd^3$ vs d for nickel in fig. 11. It can be seen that it is indeed a straight line to a high degree of accuracy. The intercept and slope for best fit produces the values of α_o and d_o:

$$\alpha_o = 4.409 \times 10^{-15} \text{ gm cm}^2/\text{sec}^2$$

$$d_o = 3.633 \times 10^{-6} \text{ cm}$$

The Van der Waals energy per unit volume is given by $V(d) = \rho g Z = \frac{\alpha_o}{d^3(1+\frac{d}{d_o})}$ This interpolation formula will be useful in later error analysis.

TABLE 1

Prediction of Lifshitz Formula for NIckel

d(Å)	Z(m)	
	ω_p = 8.3 ev	ω_p = 10 ev
200	24940	27730
300	6300	6891
400	2311	2498
500	1046	1120
600	542	576
700	309	327
800	189	199
900	122	128
1000	83	86
1100	58	60
1200	42	43
1300	31	32
1400	23	24
1500	18	18
1600	14	14
1700	11	11
1800	9	9
1900	7	7
2000	6	6

d ≡ film thickness

Z ≡ height above bath level

ω_p ≡ plasma frequency

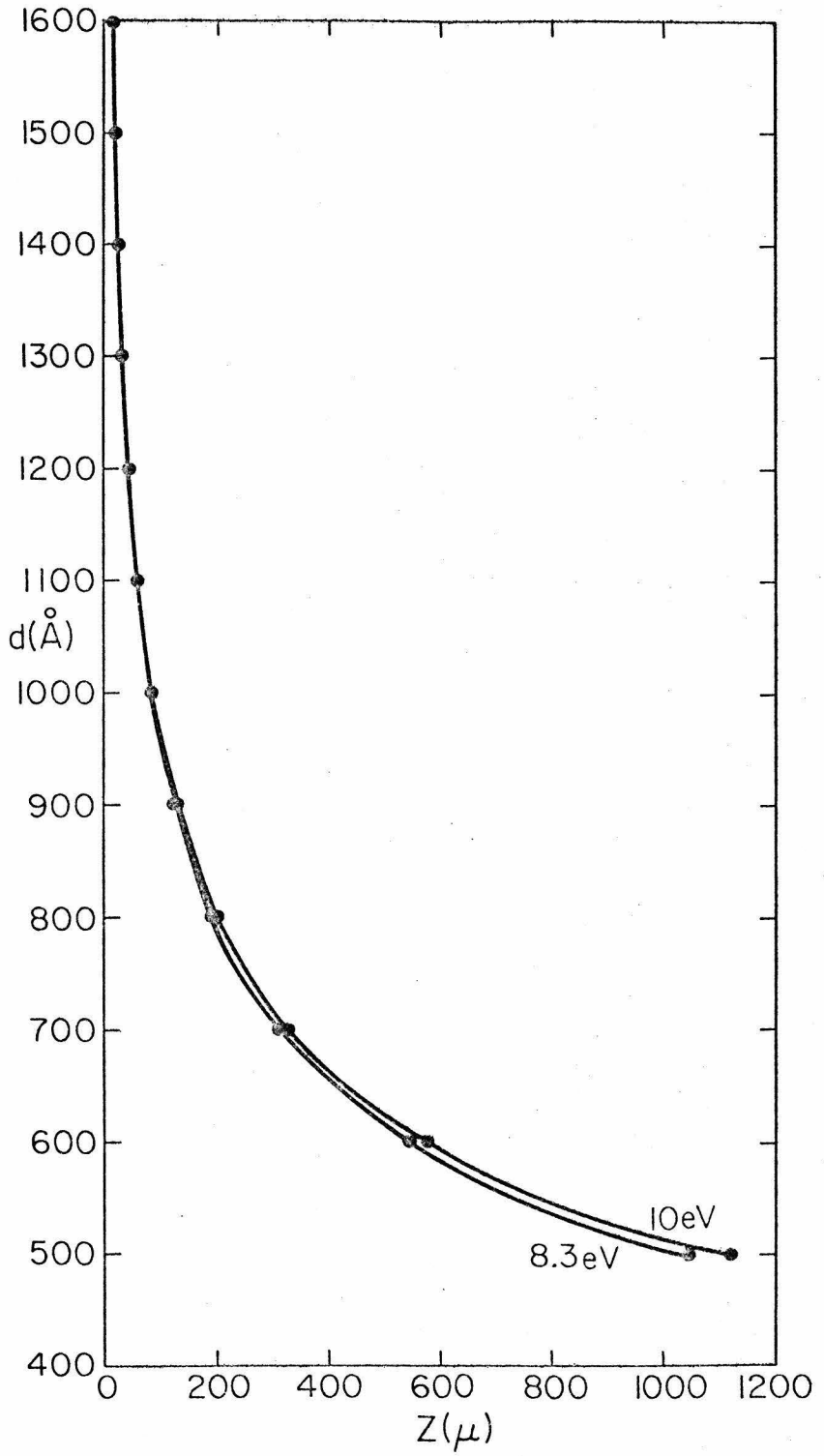

Fig. 10 Film thickness vs height above bath level as predicted by Lifshitz's theory for metals with plasma frequency of 8.3 ev and 10 ev respectively.

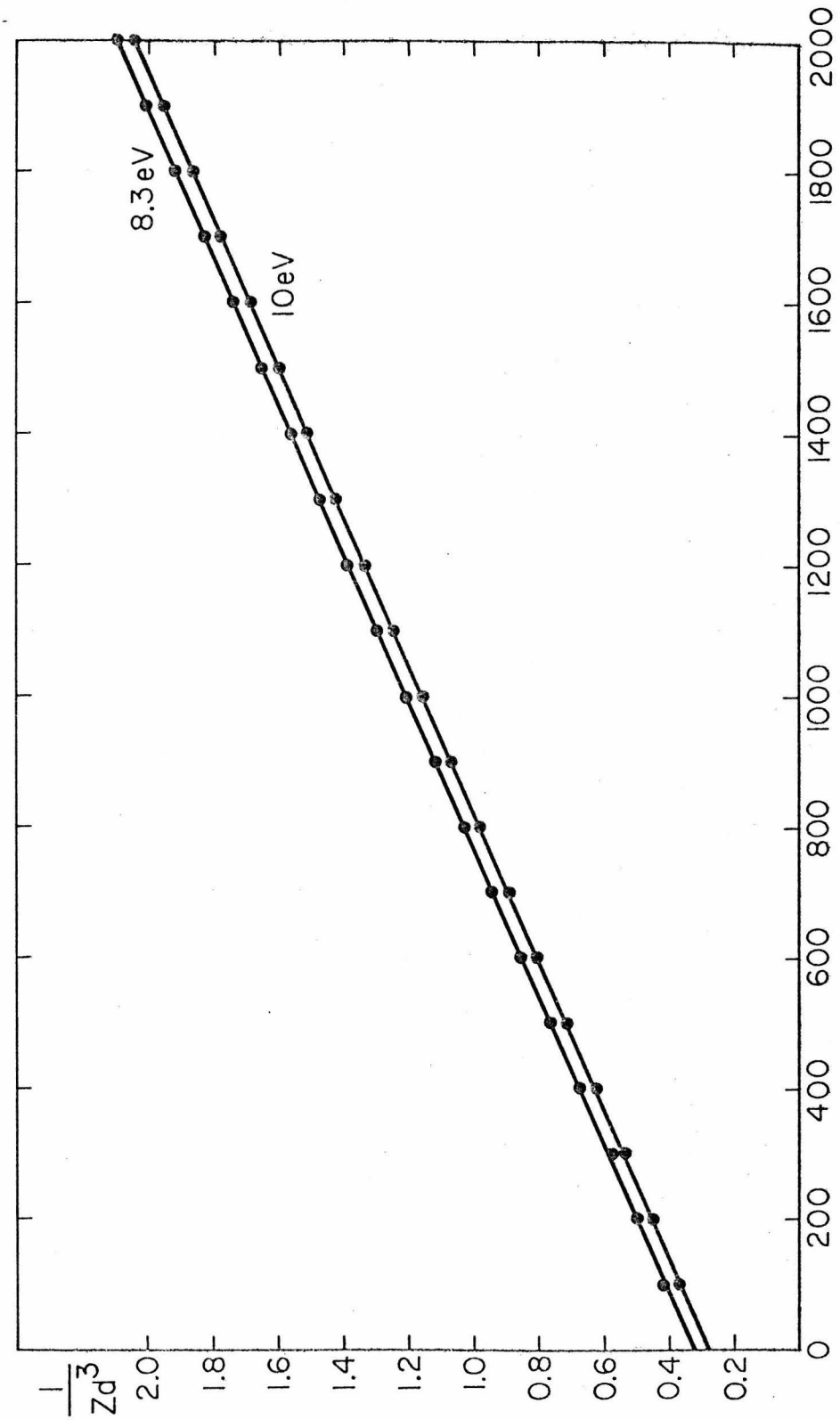

Fig. 11 Interpolation scheme for Lifshitz's formula. d = film thickness, Z = height above bath level. Points are as calculated from Lifshitz's formula. Lines are linear best fits.

II.3 METHOD

Our goal was to measure the film thickness as a function of height for super-thick films to observe the transition to the retardation regime. From fig. 10, we see that this means a height of 1 mm or lower. To get as large a range of measurement as possible, we would have to get as close to 0 mm as we can. If we again envisage using the parallel plate capacitor technique on a vertical wall, the difficulties are immediately obvious. Not only is it hard to imagine the configuration of capacitor, there are two other basic difficulties:

(i) For a vertical wall, the film profile for $z \lesssim 1$ mm would be determined more by surface tension capillary effect than by the balance between Van der Waals and gravitational force.

(ii) We have to think of a way to vary Z in an accurate manner and be able to measure it.

Difficulty (i) was solved by having a horizontal parallel plate capacitor (see fig. 12).

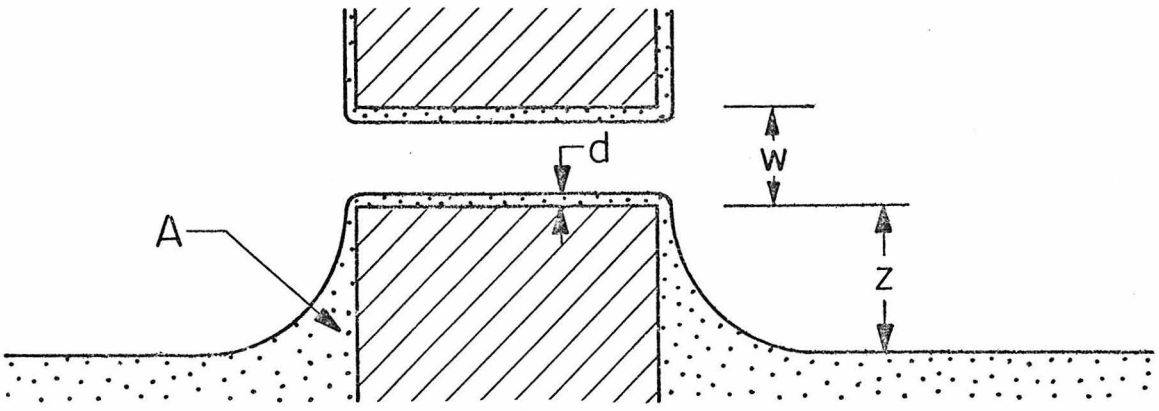

Fig. 12 Arrangement of horizontal parallel plate capacitor. d = film thickness, Z = height above bath level, w = capacitor gap.

It is easy to see that surface tension capillary effect affects the film profile in region A but not in between the capacitor plates.(Surface tension tries to minimize the area of the interface. Hence the region around A will be rounded by the effect. In between the capacitor plates, changing the film thickness will not change the interface surface area and hence the film thickness should be unaffected.) However, because of surface tension, there is question of how far away from the vertical wall should Z be measured that it be uncontaminated. Analysis shows that for Z = 1 mm, at a distance of 2 mm from the vertical wall, the error in Z is 5 μm. At a distance of 4 mm, the error in Z is 0.1 μm. So the error is small and in any event calculable.

To vary Z accurately and slowly, one obvious way is to introduce liquid into the bath by film flow from the outside. From Part I, we know that the typical flow rate is about 10^{-4} c.c./cm sec. so that if film flow is via the wall of a small tube 3mm in dia. into a bath surface of, say 10 cm^2, dZ/dt = 0.1 μm/sec. This flow rate is smaller than may be achieved by controllable needle valve.

Another way of varying Z in a virtual manner is suggested to us by M. Cole. If we have a D.C. bias electric field between the capacitor plates, the energy balance equation will now include the extra electrostatic potential energy in addition to the Van der Waals energy and gravitational energy. Instead of changing Z to change the gravitational energy, we can change the bias voltage between the plates to change the electrostatic potential energy and hence change the film thickness. For a capacitor gap of about 40 μm, changing the bias voltage from 0. volt to about 100 volt will be equivalent to changing Z from about 1 mm to 0 mm. This

idea is attractive in that the actual bath level remains constant so that we do not have to worry about any extraneous effect of a changing bath level. Secondly, we only have to measure the initial bath level Z accurately and thereafter just measure the bias voltage accurately. Thirdly, film thickness can be measured at discrete values of bias voltage whereas the film flow method would require measuring Z while Z is slowly changing.

Although the D.C. bias method sounds attractive, there are two points that have to be considered. First of all, as capacitance measurement is done by applying a small ac field across the plates (typically one to two volts) and film thickness measurements have to be accurate and remain stable to a few parts per million, it is not clear that applying a dc voltage of about 100 volt may not affect the reading, i.e. even for a bare capacitor without the helium film, it is not clear that the capacitance reading will remain the same to within a few ppm when the dc bias is turned form 0 volt to 100 volt. Whether it does depends on the quality of the capacitance bridge. Fortunately, the GR1616 capacitance bridge not only has the provision for connecting a dc bias voltage in parallel with the ac measuring voltage, it also has the stability required. The second point to be considered is that Van der Waals force is also electric in nature. It is not clear whether a strong dc bias field (100 volt across 40 μm $\simeq$ 2.5 MV/m) will affect the Van der Waals force, i.e. the bias field maybe strong enough to perturb the wave-function of the helium atom so that the Van der Waals force may become different. Perturbation analysis again shows this effect to be negligible.

Next we consider the problem of accurately measuring the initial bath level (which actually remains constant). This is again done by the

capacitance technique. The schematic representation of the experimental cell is shown in fig. 13. The body of the upper part of the cell, E, is always grounded electrically. When the film thickness is being measured, electrodes B, C and D also become grounded. Electrode A becomes the low terminal and the lower half of the cell, F, becomes the high voltage terminal. When the capacitance bridge is balanced, A is at virtual ground and as A is being surrounded by ground, the "guard-ring" effect helps to minimize edge effect. When the bath level is being measured, electrodes B, C, D are connected in parallel and become the low terminal. A is grounded and F remains the high terminal. Although the capacitance gap in this case is not small compared with the size of the capacitor (gap between B and f_2 is about 1.6 mm while B has diameter of about 5 mm), again at balance, B, C, D becomes virtual ground and because of "guard-ring" effect, the field lines between B and C are almost straight so that the increase in capacitance between B and f_2, D and f_4 etc. is linearly proportional to the depth of liquid helium. The configuration is quite similar to a 2-dimensional box where the top surface (corresponding to B and E) is grounded and the other three surfaces are at the same potential. The potential and electric field can be easily evaluated.

Finally, there remains the problem of how to maintain the cell horizontal. As the liquid level is raised in a virtual manner towards O, error of the cell being out of horizontal will introduce significant percentage error in Z for small Z. To detect if the cell is out of horizontal, we measure capacitance between BF, CF and DF in turn. The cell is attached to the He^3 refrigerator which is suspended on a frame resting on three fine-threaded screws. The screws are turned to make the readings

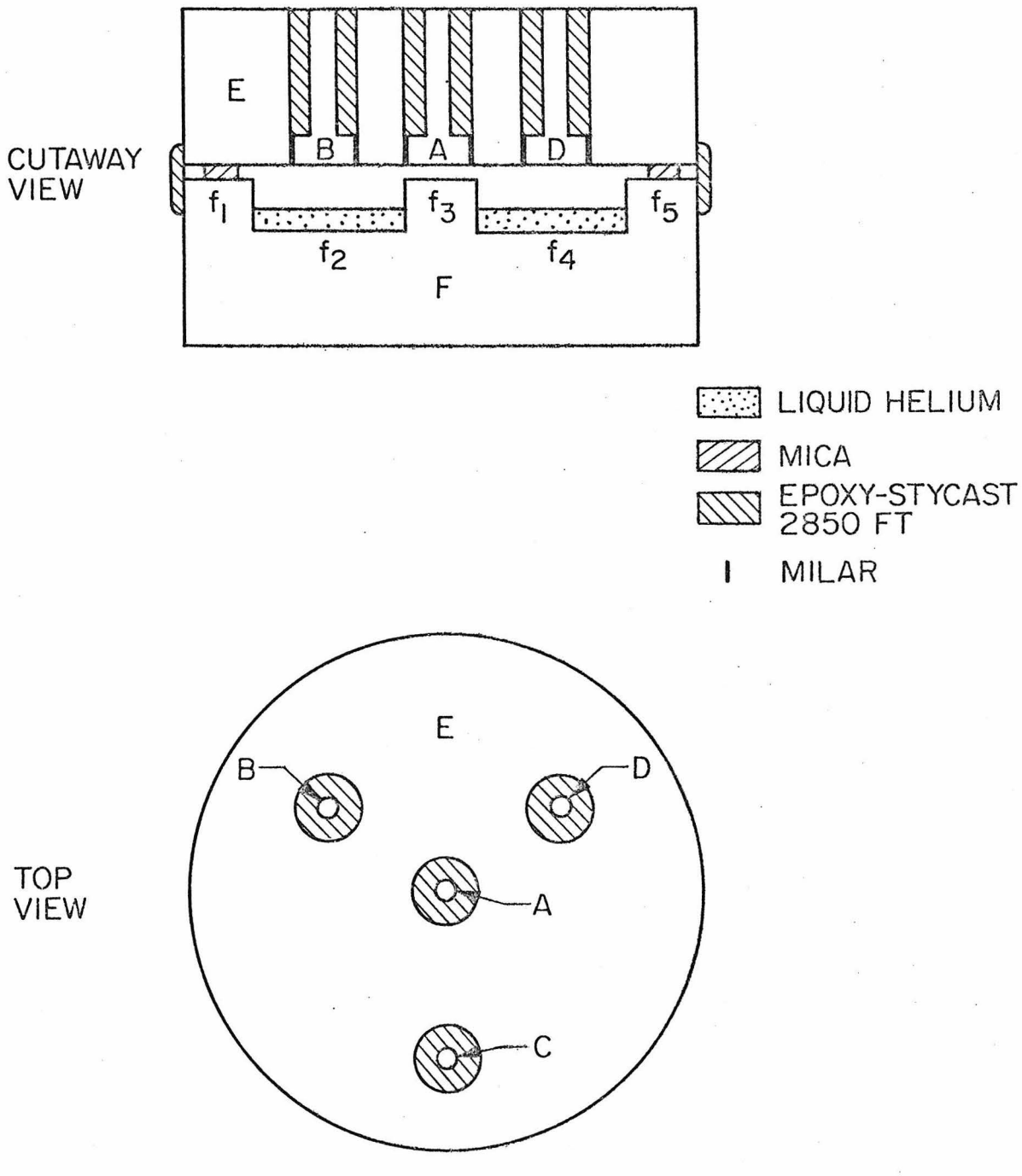

Fig. 13 Schematic representation of cell.

of BF, CF and DF equal, at which point the cell is balanced.

Details of the apparatus and experimental procedure will be discussed in the next section.

II.4 APPARATUS AND EXPERIMENTAL PROCEDURE

The experiment was carried out at a temperature less than 0.8°K so that the film capacitor measures the film thickness without the need for vapor correction. The He^3 refrigerator has been described in the INTRODUCTION. For the present experiment, some modifications are necessary. Firstly, in order to be able to balance the cell, the dewars of the refrigerator are suspended from a triangular frame resting on three 80 turn/in. screws. Secondly, to reduce mechanical vibration which may excite surface ripples in the liquid in the cell, we replace all the rigid pumping lines by flexible bellows or flexible hose so that the dewars and the cell are mechanically "isolated" from the pumps. (see fig. 14) There was concern that vibrations might be transmitted from the ground. We first tried putting an inner tube and a stack of lead bricks on top of each of the support pillars and then anchoring the fine threaded screws into the lead bricks. This is a crude vibration isolation platform. We later found the inner tubes to be quite unnecessary.

The schematic diagram of the cell has already been shown in fig. 13. We chose nickel as cell material for the following reasons: (i) It is hard enough metal (unlike aluminium or copper) that it can be machined to great precision and highly polished. (ii) It can be easily obtained in high purity (unlike brass or stainless steel). We use 99.99% purity nickel. (iii) We had in mind the possibility of repeating the experiment for a gold or copper surface by gold or copper plating the existing cell. Nickel is almost always used in preplating before gold and copper plating.

The electrodes A, B, C, D and the two halves of the cell E and F were machined separately. A, B, C, D have diameter of 4.66 ± 0.01 mm.

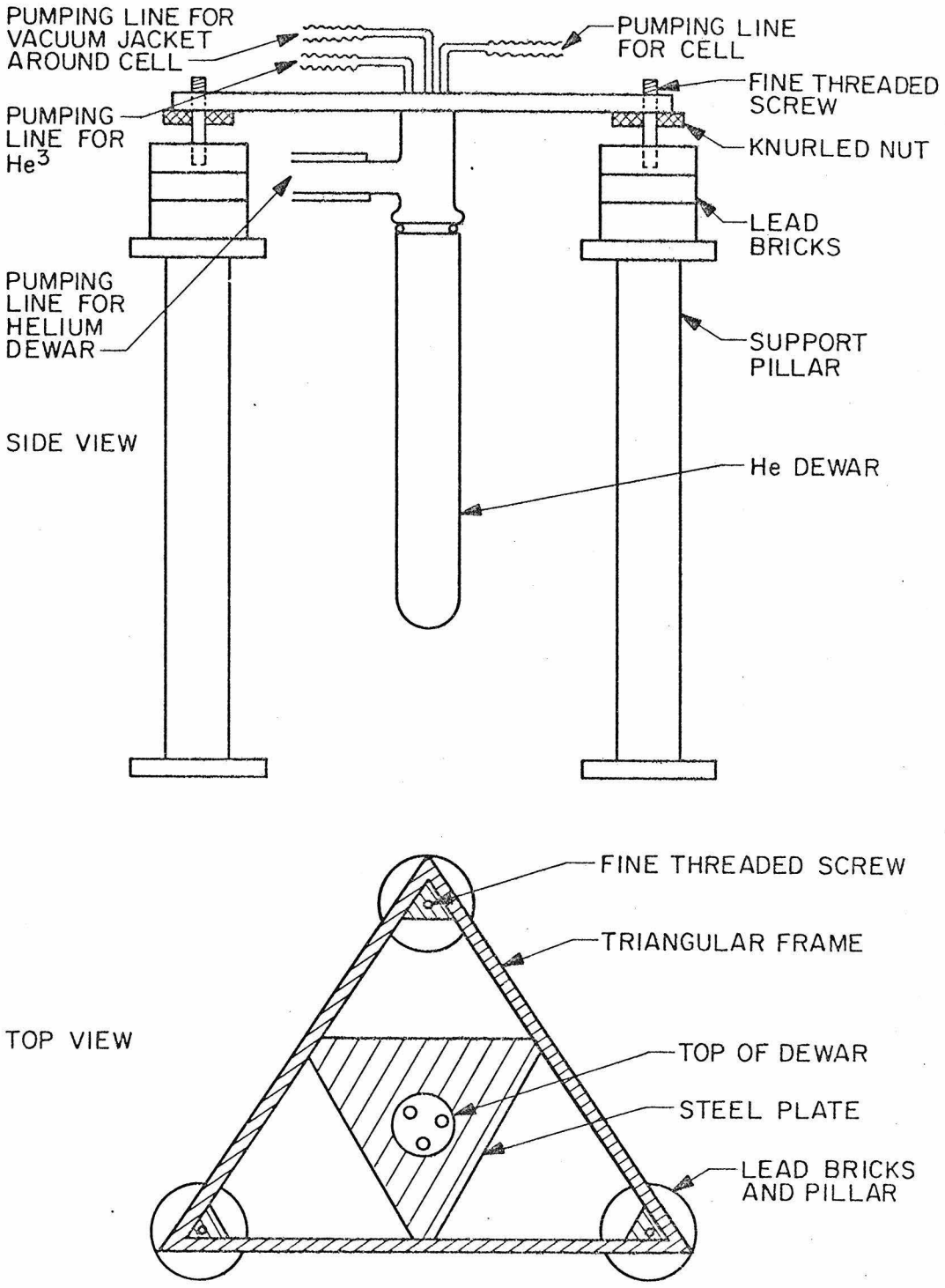

Fig. 14 He^3 refrigerator suspended on triangular frame with fine-threaded screws for balancing.

A, B, C, D were then inserted into the appropriate holes in E. The lower parts of A, B, C, D were insulated form E by mylar about 51 μm thick. The spacing between the upper parts of A, B, C, D and E were filled with the epoxy Stycast 2850FT, using catalyst 11 and cured at 75 °C. With the capacitor electrodes A, B, C, D in place, the lower surface of E was ground by a grinding machine and hand polished. The upper surface of F, $(f_1+f_2+f_3+f_4+f_5)$ was also ground by a grinding machine. $(f_1+f_3+f_5)$ was hand polished the same way as E. Polishing was done using "diamond compound" with particle size of 10 μm, 3 μm, 1 μm, 0.3 μm, 0.1 μm and finally with alumina with particle size of 500 Å. The polished surfaces were then examined under a Scanning Electron Microscope. Typical pictures of the surface are shown in fig. 15.

Measuring the capacitance between B and f_2 only determines the depth of liquid helium. To find the vertical distance between f_3 and the liquid surface, we must know the distance between f_3 and f_2 accurately. This was done by the Precision Measurement Laboratory of the Jet Propulsion Laboratory which found the distance to be 1.6358 ± 0.0005 mm. It was also found that f_1, f_3, f_5 are flat to 0.0013 mm.

The spacers between the upper half of the cell and the lower half are of critical importance because they determine how uniform the gap between A and f_3 is. Milar was first tried and found unsatisfactory because of non-uniform thickness. We next experimented with mica. Three little pieces about 38 μm thick and 2 mm x 2 mm were cut from close together on the same sheet to ensure the same thickness. They were then put on top of f_1, f_5. An optical flat was then placed on top of the spacers. Under pressure, the number of fringes could be counted to

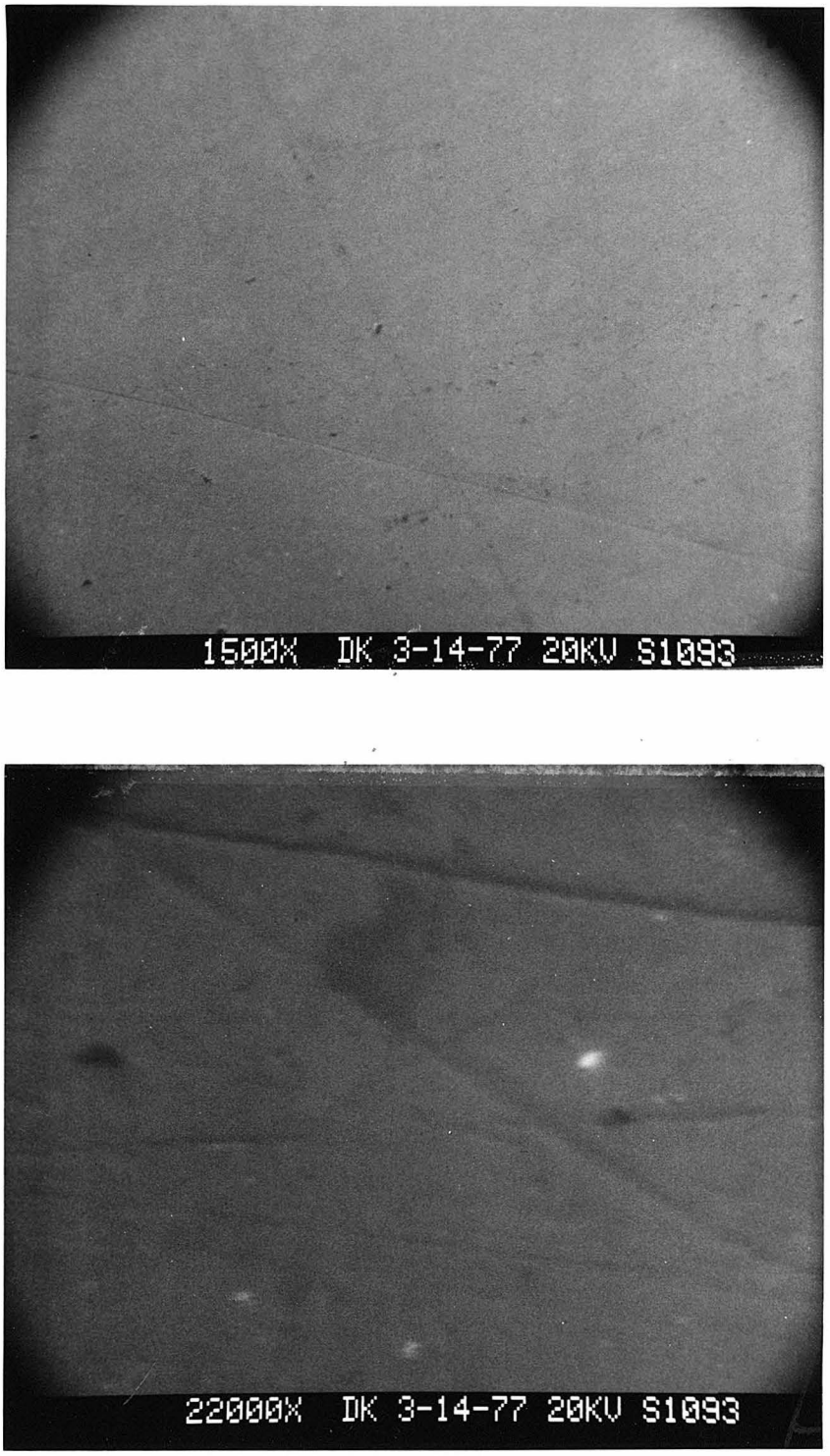

Fig. 15. SEM pictures of the cell surface at 1500x and 22000x.

determine the uniformity of separation between the bottom surface of the optical flat and f_1, f_5. It was found that about 4 - 8 fringes usually covered the surface, implying 2 - 4 μm error across the cell. Across f_3, which has a smaller area, the error would be proportionately smaller.

Before assembly, the top and bottom halves of the cell were cleaned in an ultrasonic bath with alconox, acetone, methanol and distilled water. The spacers were put in place and a 10 Kg weight put on top of the cell. Epoxy Stycast 2850FT was mixed with half its weight of fine quartz powder and with catalyst 11.(The quartz powder is used to lower the coefficient of expansion of the mixture so that it matches better with the metal.) The mixture was then applied to join the cell together. After oven curing at 75 °C for 4 hours, the cell was attached onto the refrigerator by bolts and sealed with an indium O-ring. This provides for easy disassembly and avoids contamination of the capacitor surfaces as may happen with soldering.

The cell was pumped for several days with a mechanical pump with a liquid nitrogen trap. It was also flushed several times with high purity helium gas.

A typical run was started by precooling the helium dewar overnight with liquid nitrogen. Next, liquid helium was introduced into the helium dewar and pumped down to 1.4 °K - 1.5 °K. This took about ten minutes. We let the system stand for about one hour to make sure that interior of the cell had cooled. Then "bare"readings of film capacitor Af_3 and liquid level capacitors Bf_2, Cf_2 and Df_2 were monitored. When the desired liquid level was reached, the two needle valves were turned off. This

filling process took about five to ten minutes. If the filling was done too rapidly, as might sometimes happen inadvertently (30-40 % of the time), the gap between Af_3 would fill up. In that case the cell had to be pumped to remove all traces of helium. The liquid level in the dewar by then would most likely be too low to try filling the cell, which meant we had to start the run again. After we had transferred enough liquid helium into the cell without filling the gap Af_3, we took film and level readings and started pumping the vacuum jacket around the cell (see fig. 2). During the pump down of the vacuum jacket, we balanced the cell by successively taking reading of the individual level capacitors and turning the fine-threaded screws. The pump down took about 1 to $1^1/2$ hours, at the end of which we again took readings. Then we connected the dc bias supply in parallel with the bridge detector (see fig. 16). The supply consisted of a 130 volt battery with two 10-turn pots for rough and fine adjustment of output voltage. We had tried the "precision voltage supplies" and found them unsatisfactory for two reasons: (i) for most "precision voltage supplies", output voltage could only be increased in discrete steps. These sharp jumps in voltage caused the gap Af_3 to fill prematurely when the virtual value of Z approaches zero. (ii) As the bias supply was in parallel with the bridge detector, noise from the supply would be detected. For "precision voltage supplies", this noise was equivalent to a change of film thickness of $\pm$ 30 Å. With the battery supply, the noise was about $\pm$ 10 Å and continuous variation of output voltage was possible. The 80K resistor in front of the supply was to prevent the supply from shorting the signal from point M to ground. The bias voltage was measured with a digital volt meter at point M. Since the digital volt

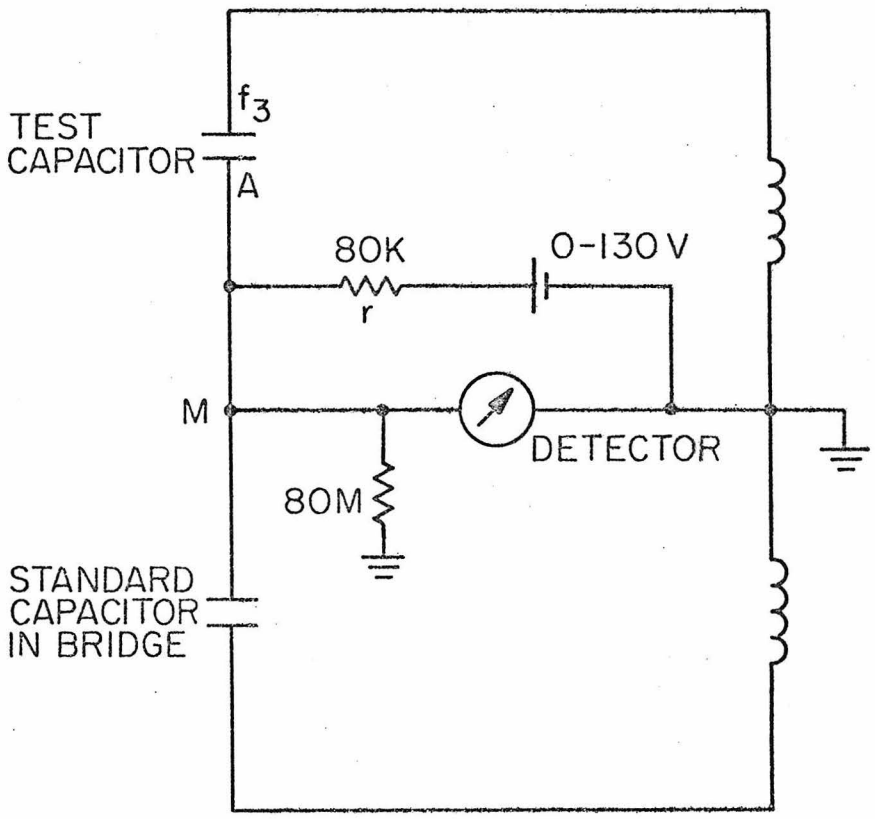

Fig. 16 Arrangement for applying dc bias voltage onto test capacitor.

meter we use only had an input inpedence of 10M for the 100 volt range, the fact that the detector had 80M input impedence had to be taken account of. This was done for all the measured voltages to arrive at the true bias voltage applied onto A.

When the dc bias supply together with the 80K resistor was connected in parallel with the detector, the phase of the bridge had to be rebalanced. However, the capacitance reading remained constant to $\pm$ 10 Å, attesting to the high quality of the GR1616 bridge.

Next we turned on the pump for the He^3 and started cooling down the cell. In about twenty minutes, the temperature would have dropped to 0.6 - 0.5 °K. The film capacitor Af_3 would also drop by 120 - 160 Å in reading, showing the condensation of helium vapor in between the plates. We waited another ten minutes and started taking the film capacitor reading. We then increased the bias voltage, let the readings stabilize, and took the reading again. The increase in bias voltage per measurement went from 30 volts at first to tens of millivolts towards the end when a small increase could change the film thickness drastically. When the voltage went higher than 100 volt, we sometimes switched back to 0 volt to check that the 0 volt reading remained constant. The end of the experiment came when the virtual level Z was about 40 μm and any further small increment in bias voltage caused the gap Af_3 to fill up. We measured this reading and started pumping the cell clean again. Then we took readings of the film and level capacitors to check their variation from their initial readings, i.e. readings taken before we opened the needle valves and filled the cell.The variation was usually quite small, of the order of 10-50 Å in equivalent film thickness, which could be totally

accounted for by the change of capacitance of the standard capacitors inside the bridge due to room temperature change over the course of the experiment. This effect can be corrected for because the temperature coefficients are known. Only on rare occasions did the readings show big jumps, of the order of 100's of Å. One explanation would be that the epoxy joints have "buckled" during the course of the experiments, as explained in Part I. This happened very rarely and on such occasions, the runs were rejected.

The total time for a typical run was eight hours at first. We later found that it could be shortened to three to four hours and produced better results because the variation of the standard capacitors would be smaller over a shorter period of time. The mechanical stability of the apparatus was good enough that on some successive runs which were a few days apart and which involved warming up to room temperature in between, the cell, after having been balanced during the first run, was found to be still in balance to within a few μm for the second run. The opening and closing of needle valves during the experiment also did not seem to affect the cell as we consistently had reading of the bare cell towards the end of a run close to the readings of the bare cell at the beginning of the run.

II.5 RESULTS AND ANALYSIS

The results of nine successful runs over a period of two months have been analysed. The initial conditions and parameters of the runs are listed in Table 2. It can be seen that after two months and numerous recyclings between room temperature and liquid helium temperature, the bare capacitance of the film measuring capacitor Af_3 changed by only about 0.7%. Initial values of Z range from 985 to 1583 μm and temperature ranges from 0.53 °K to 0.64 °K. The final value of Z, which is the last reading of the virtual level of Z before the gap of Af_3 gets filled up, is around 40 ± 10 μm (except for run no. 6 and 8).

We will discuss here how the virtual level Z and the film thickness d are obtained from our measurements of capacitance and bias voltage. Consider the situation in fig. 12, where a bias voltage V is applied between the capacitor plates and the films are in equilibrium.

Consider the change in energy of the system by moving an infinitesimal volume δv of liquid helium from the bath to the surface region of the lower film. This change is the sum of three terms:

$$\delta U = \delta U_g + \delta U_E + \delta U_V$$

where δU = change in energy of system

δU_g = change in gravitational energy

δU_E = change in electrostatic energy

δU_V = change in Van der Waals energy

δU_E corresponds to the classic problem of moving a dielectric into the gap of a capacitor.

TABLE 2

RUN NUMBER	BARE CAPACITANCE (pf)	CAPACITOR GAP (μm)	INITIAL		FINAL		TEMPERATURE °K
			Z(μm)	d(Å)	Z(μm)	d(Å)	
1	3.972000	37.933	1481	798	28	1637	0.56
2	3.971380	37.939	1554	773	40	1613	0.53
3	3.958090	38.066	1509	770	36	1641	0.53
4	3.954310	38.102	1331	822	43	1771	0.61
5	3.952690	38.118	1334	789	50	2027	0.61
6	3.942702	38.215	1583	744	89	1388	0.57
7	3.946415	38.179	1563	783	39	1910	0.56
8	3.944500	38.197	1151	869	71	1473	0.64
9	3.944240	38.200	985	911	28	1780	0.61

Since $$U_E = \frac{1}{2} CV^2 = \frac{1}{2} \frac{Q^2}{C}$$

Where C=capacitance, V=voltage, Q=charge on capacitor.

$$\delta U_E = \frac{1}{2} V^2 \delta C \qquad \text{for constant V}$$

$$= \frac{-1}{2} \frac{Q^2}{C^2} \delta C \qquad \text{for constant Q}$$

We have the classical paradox that for $\delta C > 0$ (moving dielectric into the gap), $\delta U_E > 0$ for constant V and < 0 for constant Q. The answer is of course that for constant V, the work done by the external battery has to be included. The work done = $\int V \, dQ = V^2 \, \delta C$, implying that for constant V, $\delta U_E = - \frac{1}{2} V^2 \, \delta C$ for the system alone, excluding the input of energy from the battery.

We now write out δU_g, δU_E and δU_V explicitly.

$$\delta U_g = \rho g (Z_o + d_1) \, \delta v \simeq \rho g Z_o \delta v \quad \text{since} \quad Z_o >> d_1$$

Here, ρ = density of liquid helium, g = acceleration due to gravity, Z_o = height of lower capacitor plate above bath level, d_1 = thickness of film on lower capacitor plate.

$$\delta U_E = -\frac{1}{2} V^2 \delta C$$

It is easy to show that introducing δv liquid into the gap implies

$$\delta C = C \frac{\delta v}{d_1 A} \left(\frac{\chi}{1+\chi}\right)$$

where d = gap of capacitor, A = area of capacitor, χ = dielectric susceptibility = $\frac{\varepsilon}{\varepsilon_o} - 1$, ε_o = dielectric constant of vacuum = 8.85×10^{-12} farad-meter^{-1}

Hence
$$\delta U_E = -\frac{1}{2} \frac{V^2 C^2}{\varepsilon_o} \left(\frac{\chi}{1+\chi}\right) \frac{\delta v}{A^2}$$

$$\delta U_V = -V(d_1)\, \delta v$$

where $-V(d_1)$ is the Van der Waals energy/unit volume at d_1.

At equilibrium, U = 0. Hence,

$$\rho g Z_o - \frac{1}{2} \frac{V^2 C^2}{\varepsilon_o A^2} \left(\frac{\chi}{1+\chi}\right) = V(d_1)$$

Let the L.H.S. be $\rho g Z$ where Z ≡ virtual height.

$$Z = Z_o - \frac{1}{2} \frac{V^2 C^2}{\rho g \varepsilon_o A^2} \left(\frac{\chi}{1+\chi}\right) \qquad (11)$$

Hence increasing the bias voltage is equivalent to decreasing the virtual height, as far as the film thickness is concerned. In eq. 11, all quantities on the R.H.S. are measurable experimentally, e.g. Z_o is measured initially by the capacitors Bf_2, Cf_4 etc. V is the bias voltage as measured by the digital volt meter (and corrected for the finite input impedence of of the bridge detector, as mentioned earlier). C is the bare capacitance

as measured by Af_3. A is the area of the capacitor plate A and f_3, measured under a microscope before the cell is assembled. All dimensions are corrected for contraction from room temperature to helium temperature. Similar analysis applied to the film on the upper capacitor plate shows that the change in virtual height for a given bias voltage V is the same as that for the film on the lower plate. Thus, as far as the film thickness is concerned, increasing the bias voltage is entirely equivalent to raising the bath level.

It is easy to show that the change in capacitance of Af_3 due to a film is given by

$$\delta C = C \frac{d_1}{w} \left(\frac{\chi}{1+\chi} \right)$$

where w = capacitor gap. The same equation applies for the upper film. The average film thickness is therefore given by

$$\bar{d} = \frac{d_1+d_2}{2} = \frac{1}{2} \left(\frac{\delta C}{C}\right)\left(\frac{1+\chi}{\chi}\right)w$$

$$= \frac{1}{2} \delta C \left(\frac{A\varepsilon_o}{c^2}\right)\left(\frac{1+\chi}{\chi}\right)$$

where δC is the total change in capacitance due to both upper and lower film. In trying to compare with Lifshitz's theory, we plot $\bar{d}$ vs Z for all our successful runs. Z_o in eq. 11 is measured from the mid-point between the upper and lower capacitor plates. There may be some question as to how much error we introduce by averaging the upper and lower film. Assuming Lifshitz's theory, we can see from fig.3 that at a height of 43 μm, the film thickness

should be 1200 Å whereas the mean thickness (d(62μm)+d(24μm))/2 = 1246 Å, an error of 46 Å. For a height of 60 μm, the thickness should be 1100 Å, whereas the mean measured thickness would be 1116 Å, an error of only 16 Å. Hence the error would be small except for height of 50 μm or less. In any event, this error can be estimated and corrected for.

The results of $\bar{d}$ vs Z for the nine successful runs are shown in fig. 17. It can be seen that despite the different initial bath levels and slightly different temperatures, the results coincide to within experimental error. However, it is also quickly apparent that the result is much higher than Lifshitz's prediction on fig. 3. For example, our measurement at Z = 1 mm shows a thickness of about 860 Å, about 340 Å higher than prediction. At Z = 50 μm, our measured film thickness is about 1600 Å, about 450 Å higher than predicted.

We wish to discuss here two possible sources of systematic errors which may affect our measurements. The first is due to the fact that the capacitor plates are not perfectly parallel so that the capacitor gap may be slightly narrower towards one edge. Consequently, the electric field will be slightly higher, causing the film to become thicker. We can estimate this effect as follows. Before we assemble the cell together, we found from optical means that the mica spacers have a thickness variation of 2 - 4 μm. Since the spacers are placed on the edge of the cell (surfaces f_1, f_5 in fig. 13), the variation of the gap Af_3 will be smaller by the ratio of the corresponding radii. We can thus estimate the variation across Af_3 to be $\pm$ 0.14 to $\pm$ 0.28 μm. We can put this variation into eq. 11 to find the variation in the virtual height. Eq. 11 can be written as:

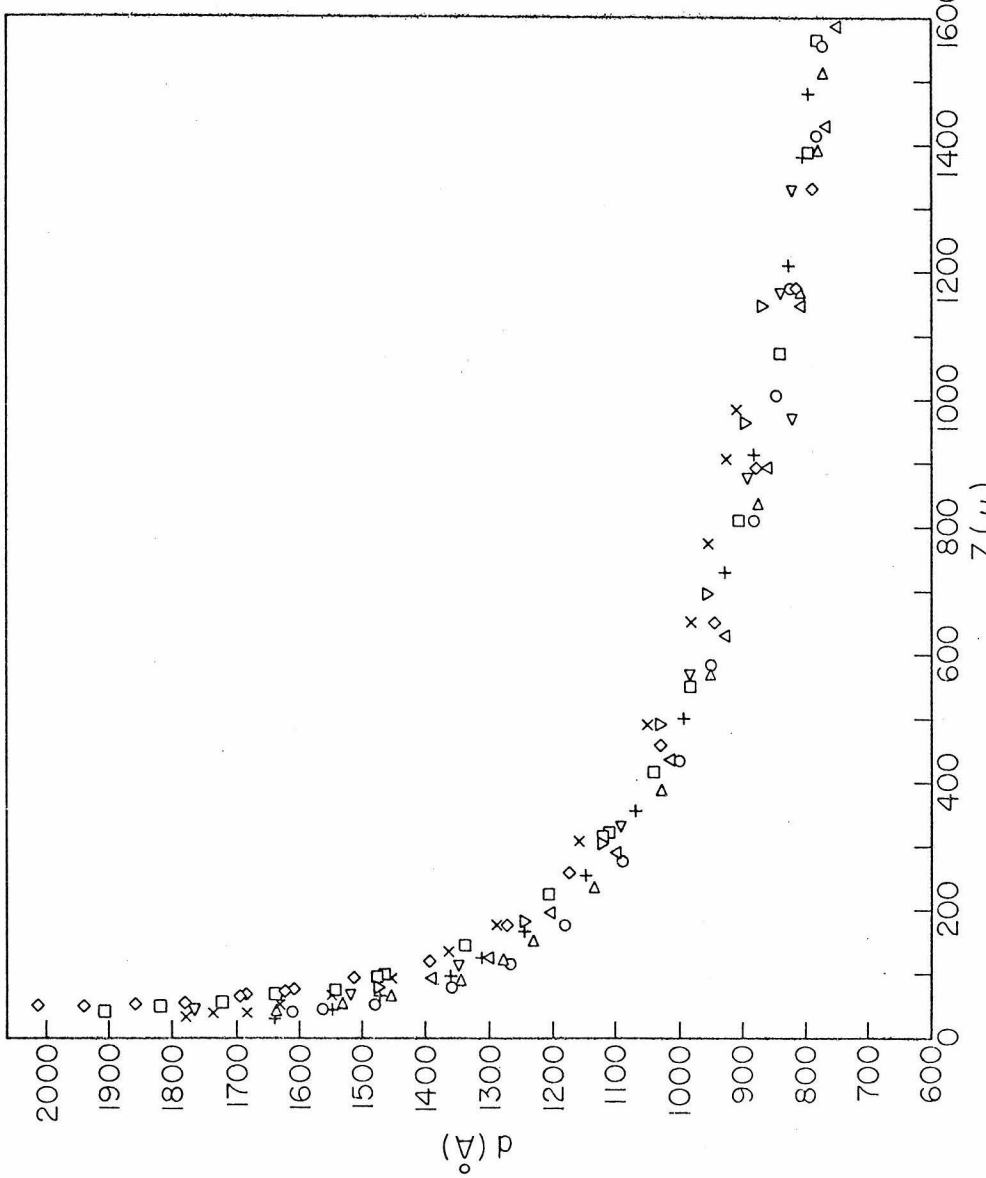

Fig. 17 Helium film thickness d vs height above bath level Z on a nickel surface. Data from nine different runs over a temperature range of 0.53-0.64 ^{o}K.

$$Z = Z_o - Z_r$$

where $$Z_r = \frac{1}{2} \frac{V^2 C^2}{\rho g \varepsilon_o A^2} \left(\frac{\chi}{1+\chi} \right) = \frac{1}{2} \frac{V^2 \varepsilon_o}{\rho g w^2} \left(\frac{\chi}{1+\chi} \right)$$

$Z_r \equiv$ the virtual rise in bath level due to the dc bias. Hence,

$$\frac{\delta Z_r}{Z_r} = -2 \frac{\delta w}{w}$$

Our mean gap $w \simeq 38$ μm. For $\delta w \simeq \pm 0.28$ μm and $Z_r \simeq 1500$ μm, $\delta Z_r \simeq 22$ μm. Thus if we start a run with $Z_o \simeq 1500$ μm and raise the virtual level by increasing V so that $Z \simeq 40$ μm, (Z referring to the mid-point between the capacitor plates) the virtual level for the lower film will be only about 21 μm. The non-uniform gap of Af_3 will cause the virtual level to be about 0 μm for one edge of the lower capacitor plate and 43 μm for the opposite edge. In such a situation, we expect the film to become so thick on one edge that it touches the upper capacitor plate. Once this happens, surface tension will cause the whole gap to fill up. In fact, this is what we observed towards the end of each run. The fact that the smallest virtual height reached is 40 ± 10 μm in all our runs seem to be consistent with our estimate of the non-uniformity of the capacitor gap. The non-uniformity of the gap not only causes the capacitor gap to fill up prematurely, it will also cause the film thickness to become thicker than expected. We estimated this error at virtual heights of 1000 μm and 60 μm. At 1000 μm, the error is less than 1 Å. At 60 μm, virtual height for the lower film is about 40 μm and film thickness at the center of the capacitor

is equal to 1200 Å. Film thickness on one edge is about 1060 Å while on the opposite edge, it is about 1520 Å. The profile of the film across the capacitor plate can in fact be estimated, using the interpolation formula of Lifshitz'z theory (fig. 11). The profile can then be integrated to give the mean thickness. In this case, the mean thickness is equal to 1220 Å, only 20 Å thicker than the "correct" value. We see that the error is close to the previously discussed error due to averaging between upper and lower films. This is reasonable as they are both due to an error in the virtual height. We estimate the sum of the two errors to be about 30 Å for virtual height equal to 60 μm and less than 1 Å for virtual height equal to 1000 μm. After correcting for the above errors, we are still left with a film thickness substantially higher than predicted. Our corrected film thickness at 60 μm is about 1520 Å, compared with 1100 Å from theory, i.e. 420 Å thicker. At 1000 μmvirtual height, our corrected film thickness is about 850 Å, about 340 Å thicker than the 510 Å predicted.

The huge discrepancy may be accounted for by the surface roughness of the capacitor plates. The last stage of our surface polishing was done with 500 Å powder in the hope that the surface roughness produced would be much less than 500 Å, and hence much less than the film thickness. If that is the case, we would expect the film thickness to be little affected by the surface roughness. However, we have no knowledge that this actually would be the case. In fact, past experiments by other investigators on helium film thickness have always led to widely varying results. This happens even for measurements using supposedly the same technique. The consensus is that different surface roughness due to different methods of surface preparation and surface treatment is the main reason for the

divergence of results.

We wish to consider here some simple models of the surface roughness and see how it affects the film thickness. Consider for simplicity the surface roughness being modelled by the rectangular wave and the sawtooth as shown in fig.18. For the case of the rectangular groove in fig. 18a, we want to find the width w smaller than which the film is more likely to fill up the whole groove by surface tension. By filling up the groove, liquid has to come from the bath and hence increases the gravitational energy. Van der Waals energy is also increased and surface energy is decreased due to the collapse of the areas A, B. At the critical w, the energy balance equation is:

$$\rho g Z r\left(\frac{w}{2} - d\right) - \int_d^{w/2} \frac{\alpha_o d_o r}{t'^4}\, dt' - \sigma = 0$$

We have assumed the Van der Waals potential is given by the interpolation formula in the retardation limit:

$$V(d) = -\frac{\alpha_o d_o}{d^4}$$

After integration and substutution of constants, the above formula gives

$$w = 370\ \mu m \qquad \text{for } z = 1.5\ mm$$

The result only serves to give a rough idea of the order of magnitude involved. As it is independent of the depth of the groove, it will only

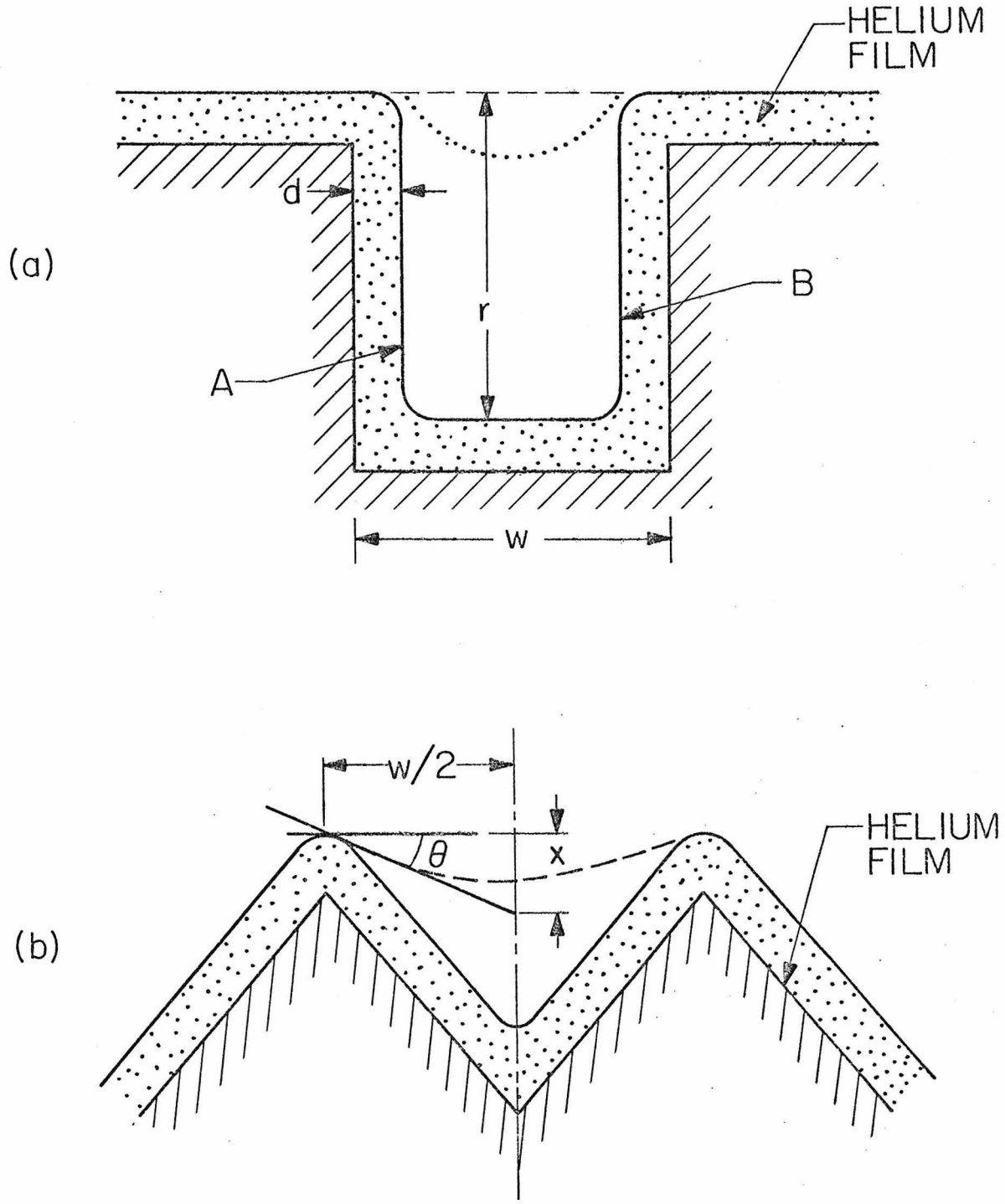

Fig. 18 Two models of surface roughness on the nickel capacitor surface.

be applicable when w is much less than the depth of the groove. For w much greater than the depth of the groove, we expect liquid to fill up along the dotted line, rather than the dashed line. Our analysis is in error because we have only shown that filling up to the dashed line lowers the energy. It may not minimize the energy.

We will try minimizing the energy for the sawtooth, which may be a little more realistic than the rectangular wave in representing surface roughness. Consider fig. 18b. We expect the liquid to fill the sawtooth along the dotted line. We will approximate this by the solid line inclined at angle θ from horizontal. From our calculation for the rectangular tooth, we know that the Van der Waals energy contributes very little in the energy balance equation so that we may drop it (the reason being that the Van der Waals energy drops off very fast beyond the normal film thickness so that for a semi-macroscopic filling as the case shown, the Van der Waals energy does not come into play). Equilibrium occurs when decreasing x by Δx causes the surface energy to drop by as much as the increase in gravitational energy,

$$\frac{1}{2}\rho g Z \Delta x \left(\frac{w}{2}\right) = -\frac{\sigma x \Delta x}{\sqrt{(x^2+(w/2)^2)}}$$

or

$$\frac{\rho g Z w}{4\sigma} = \sin\theta$$

$$\sin\theta = 14.1w \qquad \text{for } Z = 1.5 \text{ mm}$$

Thus, for example, for $\sin\theta = 0.1$, $w = 71\ \mu m$ for $Z = 1.5$ mm.

The filling in this case can be seen to be quite macroscopic. There may be question as to why surface tension does not smooth out the peaks and troughs in a symmetric manner so that there is no net increase in average thickness. The answer is of course that the peak can be lowered by at most the thickness of the film whereas the filling of the trough is limited only by the depth of the trough.

The above analysis is meant only to be qualitative. It shows that for Z = 1.5 mm, troughs of dimensions of tens of μm's already get effectively filled. Actual surface roughness of course may have troughs much smaller and shallower. A more quantitative analysis has to wait for a more quantitative description of the surface roughness. It is conceivable that the increase in mean film thickness can be calculated in terms of a Gaussian surface height distribution and a given model for the surface correlation function. We do not see fit to do this until the relevant rough surface parameters have been measured.

In summary, there are three points we have learned from the above analysis:

(i) For Z = 1.5 mm, troughs of tens of μm's can get effectively filled.

(ii) The filling is inversely proportional to Z. For example, for Z = 1.5mm, troughs less than a few μm's will get filled. The genesis of our problem maybe that our starting level of about 1.5 mm is already too small. For larger heights, surface roughness will not be as critical a problem.

(iii) The filling of troughs is equivalent to adding to the mean film thickness. Intuitively, we expect this addition to be quite constant as the film thickness increases. However, as film thickness increases,

the virtual height decreases, which will cause more troughs (troughs with bigger dimensions) to get filled, thus increasing the mean film thickness. However, if we expect the surface to have only small scale roughness, i.e. the correlation length is small and the correlation function drops off fast enough, this secondary effect may be small. This may explain why the error we observe remains relatively high and increases slightly as Z decreases. We must emphasize that all this is quite speculative.

In conclusion, we can say that all the technical difficulties connected with the measurement process can be solved. The parallelism of the capacitor gap, which limits the range of measurement for our cell to less than 1600 Å, is not a fundamental difficulty and can be improved. The feasibility of testing Lifshitz's theory for thick film on a metal surface therefore lies in the ability to prepare a clean and smooth surface. This really involves two problems: (i)good method of preparing a surface, (ii) a way of measuring and quantifying the surface roughness after the preparation to assure ourselves of a good surface. Whereas problem (i) may be solved by a careful extension of existing methods, for example, finer polishing or electroplating, we know of no good way of addressing the second problem.

PART III THE ELECTROHYDRODYNAMIC INSTABILITY OF THE SUPERTHICK HELIUM FILM

Our attempts to verify Lifshitz's theory by measuring the superthick helium film have always been hampered by one difficulty towards the end of the experimental runs - the capacitor gap fills up "prematurely" when the film thickness is only about 1600 Å thick. Although on hindsight, we can ascribe the "premature" filling to the non-uniformity of the capacitor gap, this fact was not so evident at first. We were thus led to a consideration of the possible instabilities that may exist for a superthick helium film under a strong electric field. The theoretical investigation led to the result that an electrohydrodynamic instability does exist for the film and experimental evidence shows that we may have observed it.

We first consider the simpler case of a dielectric liquid of infinite depth under a strong electric field normal to the surface of the liquid. This is a special limiting case of the capacitor geometry where the film thickness d goes to infinity and the capacitor gap w also goes to infinity while maintaining the electric field constant. Inside the fluid, the equation of motion is:

$$\rho \frac{\partial v_i}{\partial t} = \frac{\partial \sigma_{ik}}{\partial x_k} - \rho g \delta_{iz} \qquad (12)$$

where ρ = density of liquid, v_i = ith component of velicity, g = acceleration due to gravity and σ_{ik} is the stress tensor of a dielectric fluid in an electric field and is given by (24):

$$\sigma_{ik} = -p\delta_{ik} - \frac{E^2}{8\pi}(\varepsilon - \rho(\frac{\partial\varepsilon}{\partial\rho})_T)\delta_{ik} + \frac{\varepsilon E_i E_k}{4\pi}$$

where p = pressure, E = electric field magnitude, ε = dielectric constant, E_i = ith component of electric field, T = temperature. The formula is in c.g.s., in accordance with (24). Since other investigators in this field (25) also tend to use c.g.s., we will use c.g.s. in this entire development. For conversion to m.k.s. in any formula or equation, simply replace ε by $\varepsilon/\varepsilon_0$ and E by $E\sqrt{4\pi\varepsilon_0}$(26). We will state the more important results separately in m.k.s. as well.

For liquid helium where ε is only slightly greater than 1, we may take $\rho\frac{\partial\varepsilon}{\partial\rho} \simeq \varepsilon - 1$. Hence

$$\sigma_{ik} = -(\frac{E^2}{8\pi} + p)\ \delta_{ik} + \frac{\varepsilon E_i E_k}{4\pi}$$

and

$$\frac{\partial\sigma_{zk}}{\partial k} = \frac{\partial\sigma_{zz}}{\partial z} + \frac{\partial\sigma_{zx}}{\partial x} \qquad (13)$$

$$= -\frac{\partial}{\partial z}(\frac{E^2}{8\pi} + p) + \frac{\varepsilon}{4\pi}(\frac{\partial}{\partial z}E_z^2 + \frac{\partial}{\partial x}E_x E_z)$$

The electric field E_z, E_x inside the liquid will change when a small amplitude surface wave is excited. Let the original unperturbed electrostatic potential be

$$\phi_1^0 = -\varepsilon E^0 z$$

$$\phi_2^0 = -E^0 z$$

ϕ_1^0 = potential in the vapor or vacuum, ϕ_2^0 = potential in the liquid

When a small amplitude surface wave $\eta = \eta_o \sin kx$ is excited, we may write the new electrostatic potentials as

$$\phi_1 = \phi_1^o + \eta_o \mu_1 \sin kx \, e^{-kz}$$

$$\phi_2 = \phi_2^o + \eta_o \mu_2 \sin kx \, e^{kz}$$

The boundary conditions are again by

$$\phi_1 = \phi_2$$

and

$$\varepsilon \frac{\partial \phi_2}{\partial n} = \frac{\partial \phi_1}{\partial n} \qquad \text{at } z = \eta$$

where n = normal to the surface. For small η, $\frac{\partial \phi}{\partial n} \simeq \frac{\partial \phi}{\partial z}$, and the two boundary conditions give

$$-\varepsilon E^o + \mu_1 = -E^o + \mu_2$$

$$-\mu_1 = \varepsilon \mu_2$$

Hence

$$\mu_1 = \frac{\varepsilon - 1}{\varepsilon + 1} \varepsilon E^o$$

$$\mu_2 = -\frac{\varepsilon - 1}{\varepsilon + 1} E^o$$

$$\phi_1 = -\varepsilon E^o \left(z - \frac{\varepsilon - 1}{\varepsilon + 1} \eta_o \sin kx \, e^{-kz}\right)$$

$$\phi_2 = - E^o \left(z - \frac{\varepsilon-1}{\varepsilon+1} \eta_o \sin kx\, e^{kz}\right)$$

and $$E_z = E^o \left(1 + k\frac{\varepsilon-1}{\varepsilon+1} \eta_o \sin kx\, e^{kz}\right)$$

$$E_x = E_o k \frac{\varepsilon-1}{\varepsilon+1} \eta_o \cos kx\, e^{kz}$$

Dropping terms $O(\eta_o^2)$, $E_x^2 = 0$

$$E^2 = E_x^2 + E_z^2 = E_z^2$$
$$= E^{o2} + 2E^{o2} \eta_o k \frac{\varepsilon-1}{\varepsilon+1} \sin kx\, e^{kz}$$

$$E_x E_z = E^{o2} \frac{\varepsilon-1}{\varepsilon+1} k\eta_o \cos kx\, e^{kz}$$

Substituting into eq. 13, we have

$$\frac{\partial}{\partial x_k} \sigma_{zk} = - \frac{\partial}{\partial z} \left(\frac{(1-\varepsilon)E^2}{8\pi} + p \right)$$

Eq. 12 becomes $$\rho \frac{\partial v_z}{\partial t} = - \frac{\partial}{\partial z} \left(- \frac{\varepsilon-1}{8\pi} E^2 + p + \rho g z \right) \qquad (14)$$

The boundary condition to be applied at $z = \eta$ for the liquid now includes the surface tension effect. It is shown to be

$$\left(\sigma'_{ik} - \sigma_{ik} \right) n_k = \left(\alpha \nabla^2 \eta \right) n_i$$

where σ'_{ik} = stress tensor in the vapor , and α = surface tension coefficient

$$(\vec{\vec{\sigma}}' - \vec{\vec{\sigma}}) \cdot \vec{n} = -p + p_v - \frac{(\varepsilon-1)^2}{8\pi} E_z^2$$

$$p = p_v - \frac{(\varepsilon-1)^2}{8\pi} E^2 - \alpha \nabla^2 \eta \qquad \text{at } z=\eta$$

where p = pressure in liquid at interface, p_v = pressure of vapor at interface. This equation shows that not only can curvature of the surface support a pressure difference across the interface, which is well known, but also that an electric field will also introduce a force on the interface between a dielectric fluid and vacuum. The nature of this force is really quite simple. Under an electric field, the dielectric will be polarized. The net effect is equivalent to inducing a charge density inside the dielectric and a surface charge density at the surface. The interior charge density is zero if the polarization is divergenceless. The surface charge density is proportional to the polarization, and hence E. This induced surface charge is acted on by the electric field, which accounts for the E^2 factor.

Putting the above expression of p into eq. 14, eq. 14 at $z = \eta$ becomes

$$\rho \frac{\partial v_z}{\partial t} + \frac{\partial}{\partial z} \left(- \frac{\varepsilon-1}{8\pi} E^2 + p_v - \frac{(\varepsilon-1)^2}{8\pi} E^2 - \alpha \nabla^2 \eta + \rho g \eta \right) = 0$$

Assuming incompressible potential flow, $v = \nabla \phi$, where ϕ is the velocity potential.

$$\rho \frac{\partial \phi}{\partial t} - \frac{\varepsilon-1}{8\pi} \left(E^2 + (\varepsilon-1) E^2 \right) - \alpha \nabla^2 \eta + \rho g \eta = \text{constant}$$

Taking $\partial/\partial t$ and using

$$\frac{\partial E^2}{\partial t} = 2E^{o2}k\,\frac{\varepsilon-1}{\varepsilon+1}\,e^{kz}\,\frac{\partial \eta}{\partial t} = 2E^{o2}k\,\frac{\varepsilon-1}{\varepsilon+1}\,\frac{\partial \eta}{\partial t}$$

we get $$\rho\,\frac{\partial^2 \Phi}{\partial t^2} + \rho g\,\frac{\partial \eta}{\partial t} - \alpha\nabla^2\,\frac{\partial \eta}{\partial t} - \frac{(\varepsilon-1)^2}{\varepsilon(\varepsilon+1)}\,\frac{E_v^{o2}}{4\pi}\,k\,\frac{\partial \eta}{\partial t} = 0 \qquad (15)$$

where we have used $E^{o2} = \frac{E_v^{o2}}{\varepsilon^2}$. Assuming $\Phi = \Phi_o \sin kx\, e^{kz}\, e^{-i\omega t}$ and noting that $\frac{\partial \eta}{\partial t} = \frac{\partial \Phi}{\partial z}\Big|_{z=\eta}$, we get the dispersion relations:

$$\omega^2 = gk + \frac{\alpha k^3}{\rho} - \frac{(\varepsilon-1)^2}{\varepsilon(\varepsilon+1)}\,\frac{E_v^{o2}\,k^2}{4\pi\rho} \qquad (16)$$

The first two terms on the R.H.S. give the familiar "deep water wave" dispersion relations. The third term is the new effect introduced by the electric field.

A plot of the dispersion relation (actually ω^2 vs k) under various E field is shown in fig. 19. It is seen that under a strong E field, the dispersion curve bends over. At a critical E field E_{cr}, the curve touches zero at a critical $k = k_{cr}$. E_{cr} and k_{cr} are found by equating $\omega^2 = 0$ and $\frac{d\omega^2}{dk} = 0$ in eq. 16. The results are:

$$k_{cr} = \sqrt{\left(\frac{g\rho}{\alpha}\right)}$$

and

$$E_{cr} = \left(2\,\frac{\varepsilon(\varepsilon+1)4\pi}{(\varepsilon-1)^2}\,\sqrt{g\rho\alpha}\,\right)^{1/2}$$

For liquid helium, $k_{cr} = 1935/m$, $E_{cr} = 1.058 \times 10^7$ v/m and $\lambda_{cr} \equiv \frac{2\pi}{k_r}$ = 3.25 mm.

For $E > E_{cr}$, $\omega^2 < 0$, implying that the mode will grow exponentially

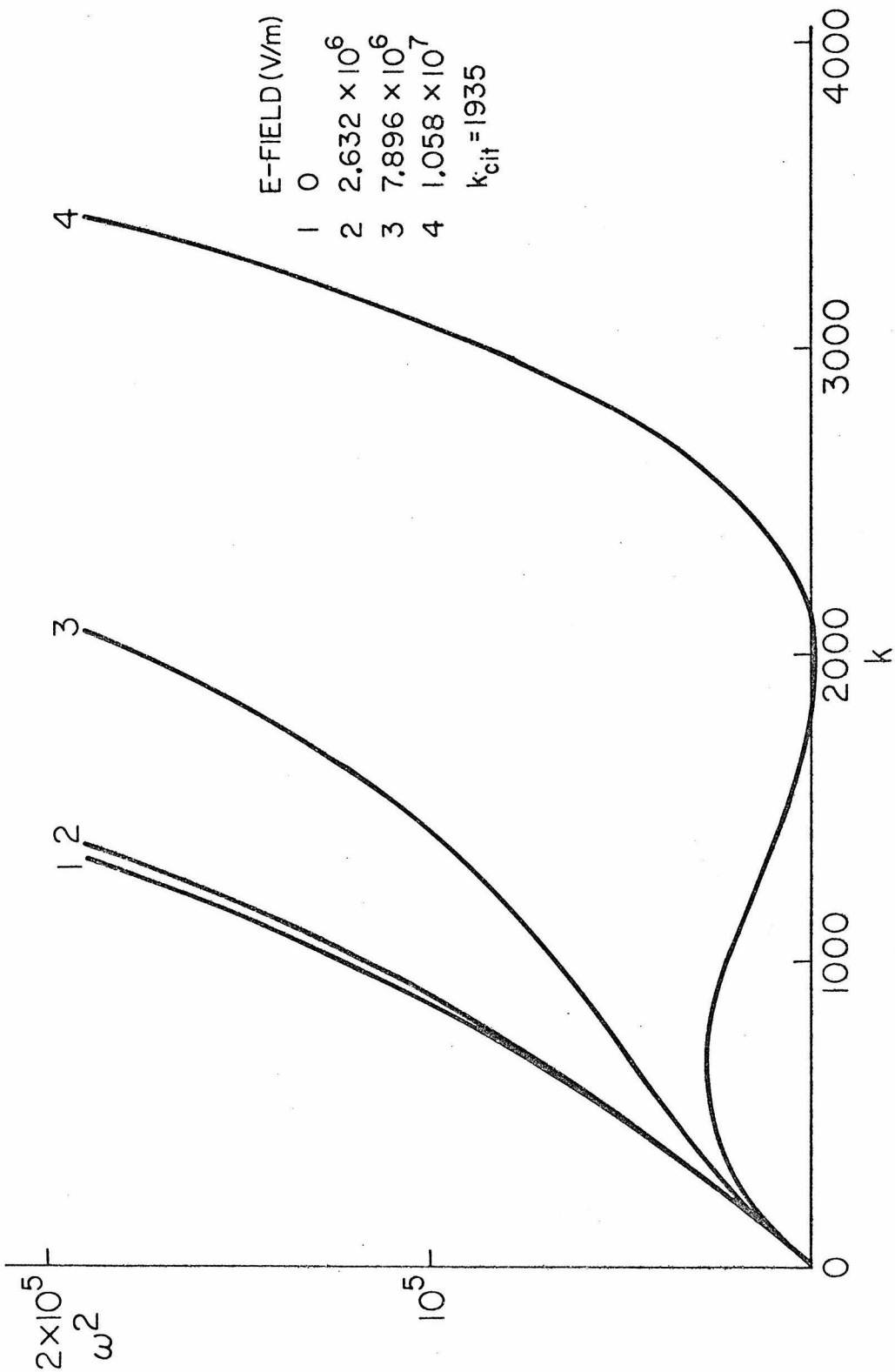

Fig. 19 Electrohydrodynamic instability for dielectric of infinite depth under a strong electric field. ω^2 becomes negative when electric field exceeds 1.058×10^7 V/m

in time which in turn implies an instability for the dielectric surface.

We now consider the case of a dielectric film in a capacitor gap. The film has thickness d, the gap has width w and the voltage is maintained constant across the capacitor plates. The approach is the same as before, although now two additional boundary conditions are imposed at the capacitor plates. The interface equation, eq. 15, uses from the electrostatics result only the fact that

$$\frac{\partial}{\partial x} E_x E_z = -\frac{1}{2} \frac{\partial}{\partial z} E^2$$

In the case of finite d, we will get the same equation if this is still true.

$$\frac{\partial}{\partial x} E_x E_z + \frac{1}{2} \frac{\partial E^2}{\partial z} = E_z \frac{\partial E_x}{\partial x} + E_x \frac{\partial E_z}{\partial x} + E \frac{\partial E}{\partial z}$$

$$= E_z \frac{\partial E_x}{\partial x} + E_z \frac{\partial E_z}{\partial z} \qquad \text{since } E^2 \simeq E_z^2 \text{ and } E_x \frac{\partial E_z}{\partial x} \simeq O(\eta^2)$$

$$= E_z \nabla \cdot E = 0$$

So we still get the equation,

$$\rho \frac{\partial \Phi}{\partial t} - \frac{\varepsilon(\varepsilon-1)}{8\pi} E^2 - \alpha \frac{\partial^2 \eta}{\partial x^2} + \rho g \eta = \text{constant}$$

We look for a solution Φ such that $\frac{\partial \Phi}{\partial z} = 0$ at $z = -d$

$$\Phi = \Phi_o e^{-i\omega t} \sin kx \cosh(k(z+d))$$

also,

$$\left.\frac{\partial \Phi}{\partial z}\right|_{\eta} = \frac{\partial \eta}{\partial t} = -i\omega\eta_o \sin kx\, e^{-i\omega t}$$

$$\frac{\partial \Phi}{\partial z} = \Phi_o\, k\, e^{-i\omega t} \sin kx \sinh(k(z+d))$$

$$= k \tanh(k(z+d))$$

$$\left.\frac{\partial \Phi}{\partial z}\right|_{\eta} = \Phi_o\, k \sin kx\, e^{-i\omega t} \sinh kd = -i\omega\eta_o \sin kx\, e^{-i\omega t}$$

$$\Phi_o = \frac{-i\omega\eta_o}{k \sinh kd}$$

$$\Phi = -i\eta_o \frac{\omega}{k} \frac{\sin kx\, e^{-i\omega t}}{\tanh kd} = \frac{-i\eta\omega}{k \tanh kd}$$

and

$$-\rho\omega^2\Phi - i\omega k^2\alpha\eta - i\omega\rho g\eta - \frac{\varepsilon(\varepsilon-1)}{8\pi} \frac{\partial}{\partial t} E^2 = 0$$

$$E_z = -\frac{\partial \Phi 2}{\partial z} = E^o - \eta\mu_2\, k \cosh(k(z+d))$$

$$E_z^2 = E^{o2} - 2E^o\eta\mu_2 k \cosh(k(z+d))$$

$$\frac{\partial}{\partial t} E_z^2 = -2E^o\mu_2 k \cosh(k(z+d)) \frac{\partial \eta}{\partial t}$$

$$= i\omega \cdot 2E^o\mu_2 k \cosh(k(z+d)) \quad \text{at the interface}$$

$$= i\omega \cdot 2E^o\mu_2 k \cosh kd$$

Equation of the interface becomes

$$i\omega\eta \frac{\rho\omega^2}{k \tanh kd} - i\omega\eta k^2\alpha - i\omega\eta\rho g - i\omega\eta \cdot 2E^o\mu_2 \, k \frac{\varepsilon(\varepsilon-1)}{8\pi} \cosh kd$$

$$\omega^2 = (gk + \frac{\alpha}{\rho} k^3) \tanh kd + E^o\mu_2 \frac{\varepsilon(\varepsilon-1)}{4\pi} k^2 \sinh kd$$

where μ_2 is determined from

$$-\varepsilon E_o - \mu_1 \sinh(k(w-d)) = -E^o + \mu_2 \sinh kd$$

and $$\mu_1 \cosh(k(w-d)) = \varepsilon\mu_2 \cosh kd$$

Here E^o is the unperturbed field in the medium. The field in the vapor is $E_v = \varepsilon E^o$. For fixed voltage V,

$$E^o = \frac{-V}{\varepsilon w - (\varepsilon-1)d}$$

We can safely take $w >> d$. Then, the boundary conditions are

$$-\varepsilon E^o - \mu_1 \sinh kw = -E^o + \mu_2 \sinh kd$$

$$\mu_1 \cosh kw = \varepsilon\mu_2 \cosh kd$$

$$E^o = \frac{-V}{\varepsilon w} = \frac{E_v}{\varepsilon}$$

$$\mu_1 = \frac{\varepsilon\mu_2 \cosh kd}{\cosh kw}$$

$$(\varepsilon-1)E^o = -\mu_2 (\sinh kd + \varepsilon\cosh kd \tanh kw)$$

$$\mu_2 = \frac{-\varepsilon(\varepsilon-1)\, E^o}{\sinh kd + \varepsilon \cosh kd \tanh kw}$$

$$\omega^2 = \left(gk + \frac{\alpha}{\rho} k^3 - \frac{(\varepsilon-1)^2}{4\pi\varepsilon\rho} \frac{k^2 E_v^{o2}}{\tanh kd + \varepsilon\tanh kw}\right) \tanh kd \qquad (16)$$

In m.k.s., $$\omega^2 = \left(gk + \frac{\alpha}{\rho} k^3 - \frac{\varepsilon_o \chi^2 k^2 E_v^2}{(1+\chi)\rho(\tanh kd + (1+\chi)\tanh kw)}\right)\tanh kd$$

To evaluate the dispersion relations numerically for a certain E_v^o, we have to find d and g first. Given an initial bath level Z_o, for any given E_v^o, we can find the virtual height Z from formula 11. Knowing Z and using the interpolation formula for the Lifshitz formula, we can find d. g is the effective g at the film surface and is given by

$$g = \pm g_o + g_v$$

where + is for lower film and - is for upper film and $g_v \equiv$ effective g due to Van der Waals force $= -\frac{1}{\rho}\frac{\partial V}{\partial d}$, where V = Van der Waals energy/unit volume Again, knowing d and using the interpolation formula, g_v and hence g can be found. Putting d and g into the dispersion relations, we can evaluate it as before. An example of this is shown in fig. 20.

Again, we want to find E_v and d at which ω^2 becomes less than zero. For our cell, d and w are extremely small so that for $kd \ll kw \ll 1$, $\tanh kd \approx kd$

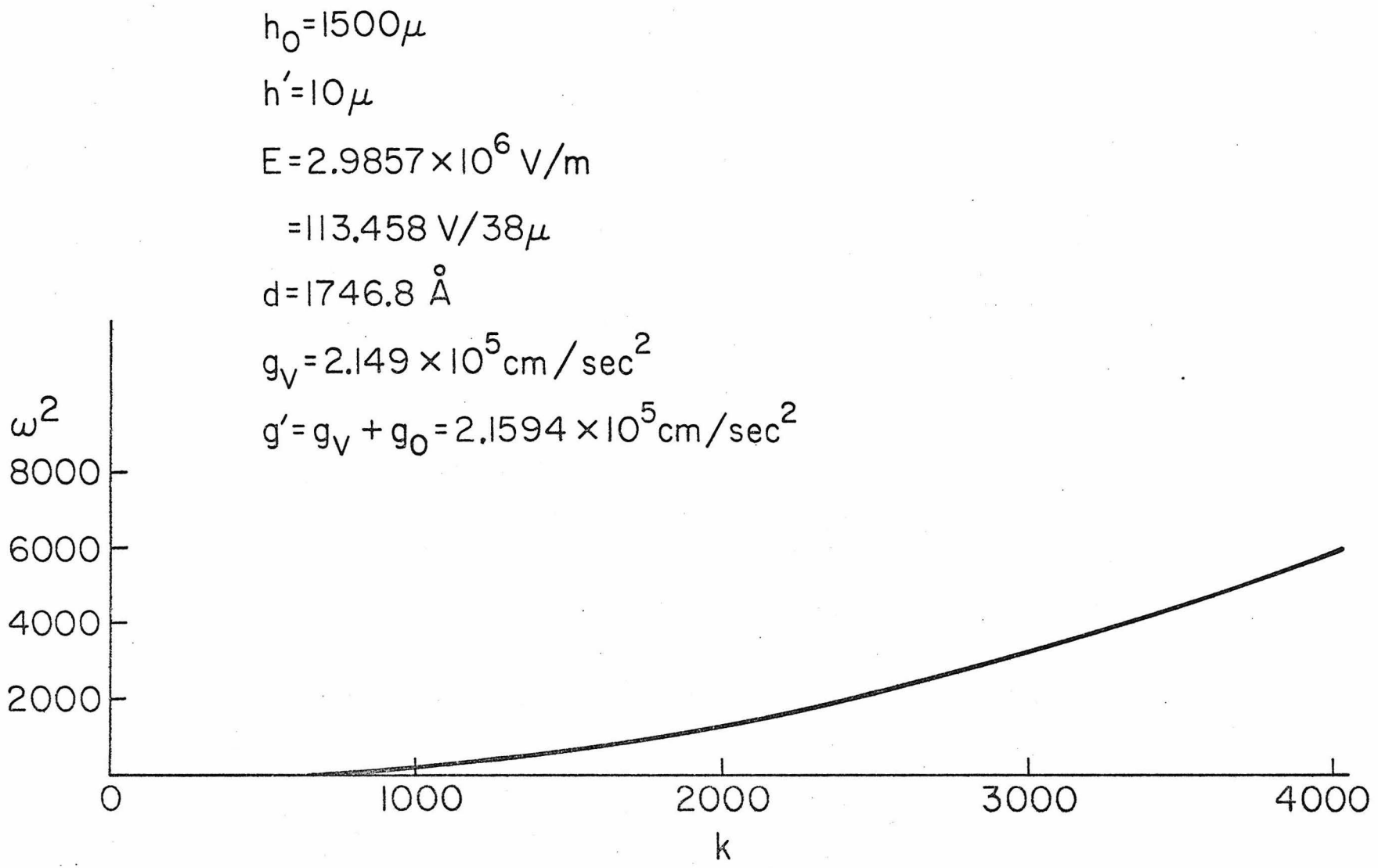

Fig. 20 ω^2 vs k for a helium film in a capacitor gap under strong electric field. Parameters are as shown.

and tanh kw ≃ kw.

$$\omega^2 \simeq \left(gk + \frac{\alpha}{\rho} k^3 - \frac{(\varepsilon-1)^2 \, k \, E_v^{o2}}{4\pi\varepsilon\rho d} \right) kd$$

therefore, $\omega^2 < 0$ when $\left(g - \frac{(\varepsilon-1)^2}{4\pi\varepsilon\rho d} E_v^{o2} \right) < 0$

The critical field is thus given by $E_v^o = \left(\frac{4\pi g \varepsilon \rho d}{(\varepsilon-1)^2} \right)^{1/2}$ (17)

The instability therefore occurs when g is effectively being cancelled by the E^2 term, at which point the net body force acting on atoms close to the surface of the fluid points away from the fluid. Surface waves with short wavelength (i.e. large k) will still be stable because the surface curvature will still provide enough restoring force. Long wavelength waves will have small curvature so that the surface tension force will be insufficient to prevent the occurrence of instability. This is the reason why long wavelength modes become unstable first.

g in eq. 17 us not a constant, but rather g = g(d(E)). We know that $E^o_{v\ crit}$ roughly has a value that would make Z = 0. So for Z_o = 1500 μm, $E^o_{v\ crit}$ ≃ 113 volt/38 μm.

$$g(d) = \pm g_o + \frac{1}{\rho} \frac{\partial V}{\partial d}$$

$$= \pm g_o + \frac{\alpha_o}{\rho} \frac{(3+4 \frac{d}{d_o})}{d^4 (1+ \frac{d}{d_o})^2}$$

where α_o, d_o are the constants in the model formula for the Van der Waals potential

$$V(d) = \frac{-\alpha_o}{d^3(1+\frac{d}{d_o})}$$

Hence eq. 17 is an equation with only d as unknown and can be solved. For the lower film, we found d_{crit} = 4170 Å. For the upper film, d_{crit} = 3780 Å.

If the capacitor gap were perfectly parallel, we would expect the lower film thickness to reach ≈ 3700 Å and then become unstable and grow to fill up the gap. For initial bath level Z_o = 1500 μm below the lower capacitor plate, a dc bias voltage of 113.862 volt would produce a virtual level of zero, i.e. film thickness would necessarily go to infinity(eq.11). A bias voltage of 113.847 volt would produce a virtual level of 0.4 μm and a film thickness of about 4000 Å. Thus to positively demonstrate that the electrohydrodynamic instability causes the gap to fill up, we have to show that the gap fills when the bias voltage is 113.847 volt rather than 113.862 volt, an error margin of only 15 mv or 0.013 %. This measurement is not impossible. However, from eq.11, we can see that the predicted voltage at which the gap fills up depends on ε, w, ρ, g so that these quantities all have to be known to accuracy much better than 0.013 %. Because of this, we think it would be quite impossible to quantitatively demonstrate the electrohydrodynamic instability of the film with our existing geometry.

However, the 15 mv error margin would allow us to qualitatively demonstrate the instability. Again, suppose that a bias voltage of 113.847 volt produces a film thickness of about 4000 Å. At any voltage

below this, the film should be stable. At any voltage up to 15 mv higher than this, the film would grow exponentially due to the instability. If we turn the bias voltage up slowly from the stable region into the unstable region, we should see the film thickness reading change from a stable reading into a "running away" condition in which the reading starts increasing exponentially in time. If the bias voltage is decreased quickly in time, the "running away" can be arrested and the film thickness reading should return to a stable value. In contrast, if the instability does not exist, there is no unstable region. Film thickness should be stable all the way up to 113.862 volt at which point the lower film touches the upper film. Once this happens, surface tension will cause the gap to be completely filled (as this minimizes the surface energy) and the process is irreversible. The existence of the instability can therefore be inferred from the existence of an unstable "window" in the bias voltage, about 15 mv wide, in which the "running away" of the film thickness and its reversibility can be exhibited.

The gap of our experimental cell is not perfectly parallel, but about 0.24 μm narrower at one edge than at the center (see Part II.5). The effect of the instability would still be roughly the same. Taking the same example as before, if the bias voltage is 113.020 volt, the film thickness at the edge would be about 4000 Å while the film thickness at the center would only be about 1250 Å (using Lifshitz's theory). At this point, instability will set in for the film at the edge region. The effect of the gap being unparallel merely causes the critical voltage for instability to be decreased from 113.847 volt to 113.020 volt, i.e. by about 0.83 volt. The "window" in which instability exists and reversibility

is possible is still about 15 mv (above 113.020 volt). In our experiment in Part II, we have indeed observed the "running away" of the film. This "running away" usually took a few seconds before it becomes irreversible and completely fills up the gap. In between, the running away could be observed to increase in an "exponential" manner with time. If the bias voltage was decreased sharply in time, the film thickness would restore to a stable value. This behaviour has been observed in several different runs. Based on this, we believe we have observed the electrohydrodynamic instability in the film. On retrospect, we can see that although the 15 mv window is small, it is still larger than the stability and resolution of our bias supply. It is this fact alone which makes the existence of the instability in the film observable.

REFERENCES

1. B. V. Rollin and F. Simon, Physica 6, 219 (1939)

2. A. K. Kikoin and B. G. Lasarew, Nature 141, 912 (1938)

3. K. R. Atkins, Proc. Roy. Soc.(London), A203, 119 (1950)

4. R. Bowers, Phil. Mag., 44, 1309 (1953)

5. E. J. Burge and L. C. Jackson, Proc. Roy. Soc.(London), A205, 270 (1951)

6. W. E. Keller, Phys. Rev. Lett. 24, 569 (1970)

7. L. Schiff, Phys. Rev. 59, 839 (1941)

8. E. M. Lifshitz, Sov. Phys. - JETP 2, 73 (1956)

9. E. S. Sabisky and C. H. Anderson, Phys. Rev. A7, 790 (1973)

10. V. M. Kontorovich, Sov. Phys. - JETP 3, 770 (1956)

11. K. Telschow, I. Rudnick and T. G. Wang, J. Low Temp. Phys. 18, 43 (1975); E. van Spronsen, H. J. Verbeek, R. de Bruyn Ouboter, K. W. Taconis and H. Van Beelen, Physica 61, 129 (1972)

12. G. M. Graham and E. Vittoratos, Phys. Rev. Lett. 33, 1136 (1974)

13. D. L. Goodstein and P. G. Saffman, Phys. Rev. Lett. 24, 1402 (1970); Proc. Roy. Soc.(London), A325, 447 (1971)

14. D. L. Goodstein and P. G. Saffman, J. Low Temp. Phys. 18, 435 (1975)

15. E. van Spronsen, H. J. Verbeek, R. de Bruyn Ouboter, K. W. Taconis and H. van Beelen, Phys. Lett. A45, 49 (1973)

16. G. A. Williams and R. E. Packard, Phys. Rev. Lett. 32, 587 (1974)

17. K. R. Atkins, Proc. Roy. Soc.(London), A203, 119, 240 (1950)

18. F. London, Z. Physik 63, 245 (1930)

19. H. B. G. Casimir and D. Polder, Phys. Rev. 73, 360 (1948)

20. I. E. Dzyaloshinskii, E. M. Lifshitz and L. P. Pitaevskii, Advanc Phys. 10, 165 (1961)

21. V. B. Derjaguin and I. I. Abrikossova, Discussions Faraday Soc. 18, 33 (1954)

22. J. A. Kitchener and A. P. Prosser, Proc. Roy. Soc.(London), A242, 403 (1957); W. Black, J. G. V. de Jongh, J. Th. G. Overbeek and M. J. Sparnaay, Trans. Faraday Soc. 56, 1597 (1969)

23. V. A. Parsegian and B. W. Ninham, J. Chem. Phys. 52, 4578 (1970)

24. L. D. Landau and E. M. Lifshitz, Electrodynamics of Continuous Media, Addison-Wesley, Reading, Mass, 1960, pp.64-69

25. E. A. Kuznetsov and M. D. Spektor, Sov. Phys. - JETP 44, 136 (1976) and references therein; G. I. Taylor and A. D. McEwan, J. Fluid Mech., XXII, 1 (1965)

26. J. D. Jackson, Classical Electrodynamics, Wiley, N.Y., 1963, p.619

27. NBS Handbook of Mathematical Functions, Ch. 25

28. L. I. Schiff, Quantum Mechanics, McGraw-Hill, N.Y., p.260